DESIGN OF A PV SYSTEM INCLUDING ITS SCADA FOR A HOUSE IN IRAN

by
© ATEFEH ZARE

A thesis submitted to the School of Graduate Studies in partial fulfillment of the requirements for the degree of

Master of Engineering

Faculty of Engineering and Applied Science
Memorial University of Newfoundland

May 2021

St John’s, Newfoundland, Canada

Abstract

Solar Radiation in the Middle East is relatively high and is one of the most sustainable renewable sources. However, Iran has not utilized it as one of the most significant sources of energy yet. Considering the mentioned concern, in this Thesis, a PV system is designed using BEopt and Homer software for a house in Golpayegan, Iran. Thermal modeling of the house is done using BEopt software to determine the hourly load consumption profile. The meteorological data and the generated hourly load data are used by Homer software to size the system based on the optimum net present cost. The cost analysis results demonstrate that the PV/grid is the most optimal solution for the under-consideration house. Then a control strategy is proposed to connect the suggested PV system to the electric distribution grid. The proposed control strategy aims to design the Maximum Power Point Tracking (MPPT) algorithm and control the injected active and reactive PV arrays power. The reactive power control provides the PV system with Power Factor Correction (PFC) capability, improving the system's overall performance. Finally, in the last phase of research, a secure, reliable, low-cost, and open-source SCADA system is developed using the most recent SCADA architecture, the Internet of Things. The proposed SCADA system prototype is implemented and tested to measure the temperature, humidity, pressure, and light intensity of a house and control smart home appliances. The results show that the developed open-source SCADA system performs optimally and accurately and could serve as a viable control and monitoring system for PV applications by minor changes.

Acknowledgements

First of all, I would like to express my sincere gratitude to my supervisor Prof. M. Tariq Iqbal for the continuous and timely support of study and research, I greatly appreciate his instruction, patience, motivation, enthusiasm, and immense knowledge.

I would like to thank my sister who supported me with financial support from her company Pooya Pajouhan Nirouye Golpa Co., which enabled me to finish my graduate study.

I like to thank the School of Graduate Studies, Faculty of Engineering and Applied Science, and my friends.

Finally, I also want to send my acknowledge to my beloved family, who have been giving me their kindness and emotional support.

Table of Contents

List of Figures

List of Tables

List of Abbreviations and Symbols

SCADA	Supervisory Control and Data Acquisition
IoT	Internet of Things
HMI	Human Machine Interface
PLC	Programmable Logic Controller
MTU	Master Terminal Unit
RTU	Remote Terminal Unit
API	Application Programming Interface
PV	Photovoltaic
MQTT	Message Queuing Telemetry Transport
MPPT	Maximum Power Point Tracking
HPS	Hybrid Power System
RES	Renewable energy System
HOMER	Hybrid Optimization of Multiple Energy Resources
BEOpt	Building Energy Optimization
PI	Proportion Integration
P&O	Perturbation and Observation

SOC	State of Charge
PCC	Point of Common Coupling
PFC	Power Factor Correction
STC	Standard Test Conditions
NASA	National Aeronautics and Space Administration

Chapter 1: Introduction and Literature Review

1.1 Development of Renewable Power Systems in Iran

Worldwide energy demand has grown by 2.9% in 2018, almost doubling its 10-year average from 2007 to 2017, the highest level since 2010 [1]. Due to this increase in energy demand and more fossil fuel consumption, global warming has become one of the biggest human problems. In recent years, public awareness, the number of communities, and national and international global warming meetings have increased. Prominent examples of international meetings include the Paris Agreement [2] and the Kyoto Protocol [3], the two most critical UN conventions on climate change.

Global carbon emissions caused by energy consumption have risen by 2.0% in 2018, which is the highest level for the last seven years, with a carbon emission of about 0.6 gigatons. Significantly, the increment in carbon emission is a direct result of grown energy consumption [1]. Considering the vital role of coal in carbon emission, more countries are obligated to move away from coal consumption for electricity generation (e.g., Canada, France, etc.) [5, 6] or do not allocate more funds for the use of coal (for example, Brasilia) [7]. However, opposing these efforts, several countries stated plans to develop coal production and utilization [4]. However, in 2018 there was a significant return to coal production (4.3) and consumption (1.4) [1].

In many countries, the emission portion for each power company is limited. With the emission trading model, they can determine the best solution after achieving a set of Pareto

solutions related to different distribution portions. This technique is economically beneficial for countries with this ability [8,9]. Renewable energy markets faced some challenges because of low coal and natural oil and gas prices, especially in the heating and transportation sectors [10,11]. Fossil fuel subsidies, which remain significantly higher than renewable energy subsidies, continue to influence renewable energy development. In 2017, more than 50 countries agreed to eliminate fossil fuel subsidies due to international commitments [12]. Similarly, subsidy amendments got implemented in 2016 in several countries such as Brazil, India, Iran, Egypt, Nigeria, Saudi Arabia, Sierra Leone, Tunisia, Thailand, Ukraine, and Venezuela [13].

Since 2019, many countries have been directly and indirectly supporting the development and deployment of renewable energy to achieve technological advances, reduce costs, and increase the use of renewable energy sources. In those countries, authorities are working to integrate renewable energy into their conventional national energy systems.

Iran, an Asian country, is the 18th largest and 17th most populous country in the world [14]. Population growth has increased the need for more energy production. However, the required electricity is mainly generated from fossil fuel sources. Iran has the second proven natural gas reserves (33.5 trillion cubic meters) and the fourth proven crude oil reserves (158.4 thousand million barrels) in the world, which is about 18% and 9.3% of the world's total reserves, respectively [15, 16]. In addition to its enormous reserves of fossil fuels, Iran has excellent potential for using renewable energy sources e. g., solar, wind,

hydropower, biomass, and geothermal. Thus, authorities have established supportive policies to encourage people to utilize clean energy sources.

Today, solar energy, as a significant source of energy, has attracted much attention. It can be utilized using solar thermal and PV technology [17]. PV devices or solar cells convert sunlight energy into electricity without producing pollution or moving parts. A PV system works differently from most power generation systems because of its automatic operation [18,19]. These systems are modularly produced and can be developed on different scales. Solar energy is extensively available in most parts of Iran, especially in the southern and central regions (Fig.1). The radiation pattern changes between 2.8 kWh/m2 in the southeast to 5.4 kWh/m2 in the central parts. In a radiation analysis in the whole country, it is estimated that in 80% of Iran's area, solar radiation is between 1640 to 1970 kWh/m2/year [20-22].

Although the potential for solar energy harvesting in Iran is relatively high, various factors such as the low price of fossil fuels in electricity generation and the high expenses of PV devices have led to the limited development of PV technology in Iran. However, new supportive policies have been developed to stimulate renewable energy use and turn them into competitive technologies with conventional electricity generation sources. These policies make renewable energy more affordable for the people who live there [23].

Annually, due to the 30-40% growth of the PV market, PV technology becomes one of the most appropriate energy carriers [24].

1.2 System Sizing for PV Power Systems

PV system sizing aims to design an economically reliable system based on local meteorological weather data and hourly load data. To estimate the hourly load data for the selected location, the site's thermal modeling can be done to estimate how to load data. Free BEopt software is used for thermal modeling of the house [25]. The purpose of optimum system sizing is to minimize the Net Present Cost and Levelized Cost of energy. There have been many software programs to accomplish this purpose; HOMER has been the most practical and functional one. HOMER economically determines the optimal design and examines the system's feasibility regarding users' requirements and the registered data [26].

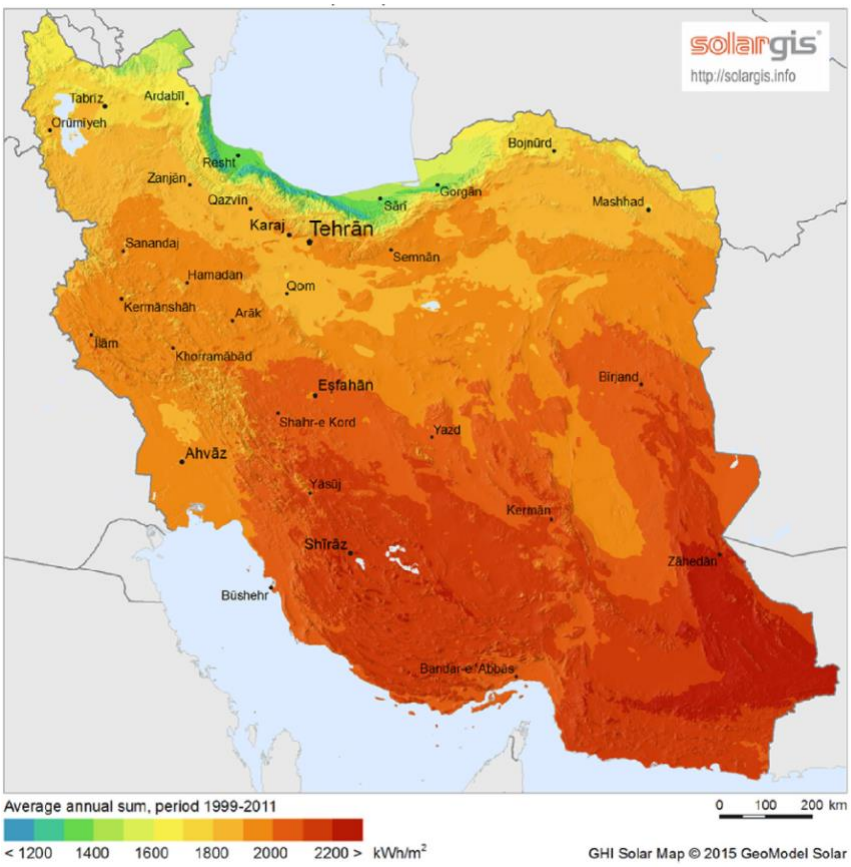

Fig. 1-Global horizontal irradiation (GHI) in Iran [24].

1.3 Dynamic Modeling and Simulation of Hybrid Power System

The dynamic modeling examines the designed system's transient dynamic under different possible inputs and disturbances. The PV power system's dynamic model comprises a dynamic model of each component and control system designed to maintain the entire system stable. The grid-connected PV solar system consists of PV panels, a voltage source converter (VSI), and a filter that is usually part of the VSI. Fig. 2 shows a grid-connected PV power system.

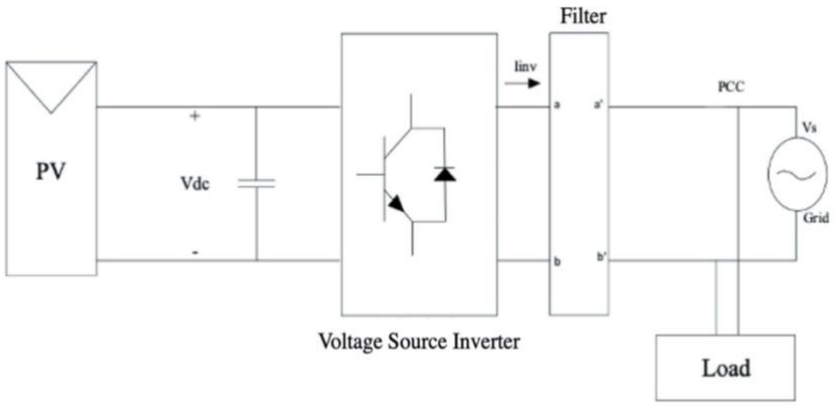

Fig. 2-Grid connected Photovoltaic Solar System.

PV arrays consist of series/parallel connections of some PV modules, where a module comprises a series connection of several PV cells. The PV Solar arrays are connected in parallel to the dc-link capacitor, C, and the DC side terminals of the VSI. The primary function of the dc-link capacitor is to maintain a constant DC bus voltage. The VSI is the core of the grid-connected PV system that transforms DC power from the PV arrays into AC power via a set of solid-state switches such as IGBTs [27]. The switching action of these semiconductor valves is governed by the control system implemented in a microcontroller on the VSI inverter [28]. The filter keeps harmonic currents at low levels and ensures a low voltage distortion at the PCC [29].

1.4 Supervisory Control and Data Acquisition

Supervisory Control and Data Acquisition (SCADA) is a technology that enables a user to receive data from one or more remote facilities and/or send limited control instructions to them. SCADA's primary function is for acquiring data from remote devices located in

the remote location in a wide range of industrial and residential utilization providing overall control remotely from a SCADA Host software platform [30].

Home automation systems using SCADA consists of four major parts. The first part is the sensing devices placed at several locations throughout the home to measure the desired variables. The second part is Remote Terminal Units (RTUs) for acquiring remote data from sensors. The third one is Master Terminal Units (MTUs) to process the received data and deal with Human Machine Interfaces (HMI) [31]. The last part of SCADA is the communication channel to connect the RTUs to the MTUs [32].

Research communities worldwide have been working on improvements of SCADA systems and using a combination of open-source hardware, servers, software, and IoT platforms. They have offered numerous open-source remote monitoring and control solutions such as PLC-Based [33] systems, PIC Micro-Controller-Based systems [34], PC-Based systems [35], ESP8266-Based systems/Web-based Wireless Sensor Solutions [36], and Arduino-Based Systems [37].

1.5 Research Objectives

To deal with the difficulty of utilizing solar energy in Iran, this thesis objectives are listed below:

I. To design a reliable PV power system for a household in Iran based on the weather data, estimated load data, and building construction. Size the designed system for the most optimum design and least system cost.

II. To build a dynamic model of the final sized system in Simulink/MATLAB and develop a control system to keep the system model operating at the best functionality.

III. To simulate the designed dynamic model under various circumstances and analyze its transient dynamic based on the simulation results.

IV. To design a low-cost and open-source SCADA system to acquire desired parameters, remotely monitor them, and launch supervisory control actions using the developed human-machine interface (dashboards) on the chosen IoT platforms.

1.6 Thesis Organization

A manuscript style format has been adopted in the preparation of this thesis. A summary of the thesis and each of the chapters is presented as follows:

Chapter 2 presents the design and analysis of a Photovoltaic (PV) system to supply the residential load of a house in Golpayegan, Iran. Thermal modeling of the house is done using BEopt software to determine the hourly load profile. Then primary meteorological data of solar irradiance and temperature for the selected site and estimated load data are used by HOMER software to optimize the system sizing for PV/grid and PV/diesel/battery models. This chapter's work has been submitted to the 2020 IEEE International Conference on Smart Communities and is under revision.

Chapter 3 presents the control strategy design to connect the sized PV system to the electric distribution grid. This chapter focuses on controller design for a single-phase grid-connected PV system and its implementation for power factor correction in the distribution power system to enhance the designed renewable energy system's overall performance. This chapter's work has been submitted to the 2020 IEEE International Conference on Smart Communities and is under revision.

Chapter 4 presents a low-cost, open-source, and reliable Supervisory Control and Data Acquisition (SCADA) system for home monitoring and control system. The presented SCADA system consists of analog sensors, ESP32, Node-RED, and Message Queuing Telemetry Transport (MQTT) through local Wi-Fi to remotely access and controls the home appliances. This chapter is a paper that has been published at the 2020 IEEE International IoT, Electronics, and Mechatronics Conference (IEMTRONICS).

References

[1] Statistical Review of World Energy | Energy economics | Home", bp global, 2020. [Online]. Available: https://www.bp.com/en/global/corpora-te/energy-economics/statistical-review-of-world-energy.html.

[2] Unfccc.int, 2020. [Online]. Available: http://unfccc.int/paris_agreement/items/9485.php.

[3] Unfccc.int, 2020. [Online]. Available: https://unfccc.int/process-and-meetings/the-kyoto-protocol/what-is-the-kyoto-protocol/kyoto-protocol-targets-for-the-first-commitment-period.

[4] "Canada set to phase out coal-fired power by 2030", The Independent, 2020. [Online]. Available: https://www.independent.co.uk/news/world/americas/canada-renewable-energy-catherine-mckenna-coal-fired-power-2030-a7430471.html.

[5] France is shutting down all coal-fired power plants by 2023", The Independent, 2020. [Online]. Available: https://www.independent.co.uk/news/world/europe/france-close-coalplants-shut-down-2023-global-warming-climate-change a7422966 .html.

[6] M. Teixeira, "UPDATE 1-Brazil development bank scraps financing for coal-fired plants", CA, 2020. https://ca.reuters.com/article/ idUSL2N1C913N.

[7] H. Khaloie et al., "Coordinated wind-thermal-energy storage offering strategy in energy and spinning reserve markets using a multi-stage model", Applied Energy, vol. 259, p. 114168, 2020. Available: 10.1016/j.apenergy.2019.114168.

[8] H. Khaloie et al., "Co-optimized bidding strategy of an integrated wind-thermal-photovoltaic system in deregulated electricity market under uncertainties", Journal of Cleaner Production, vol. 242, p. 118434, 2020. Available: 10.1016/j.jclepro.2019.118434.

[9] I. Shah, C. Hiles and B. Morley, "How do oil prices, macroeconomic factors and policies affect the market for renewable energy?", Applied Energy, vol. 215, pp. 87-97, 2018. Available: 10.1016/j.apenergy.2018.01.084.

[10] "Natural gas | Energy economics | Home", bp global, 2020. https://www.bp.com/en/global/corporate/energy-economics/statistical-review-of-world-energy/natural-gas.html.

[11] I. Gerasimchuk, Fossil-Fuel Subsidy Reform: Critical Mass for Critical Change. 2015.

[12] "Global Subsidies Initiative", Global Subsidies Initiative, 2020. [Online]. Available: https://www.iisd.org/gsi/.

[13] N. Norouzi, M. Fani. "The seventh line: a scenario planning strategic framework for Iranian 7th energy progress plan by 2020-2025." Energy Management and Technology Journal 5.3, 2021.

[14] https://en.wikipedia.org/wiki/Iran

[15] G. Ghasemi, et al. "Theoretical and technical potential evaluation of solar power generation in Iran." Renewable Energy 138, 2019.

[16] S. Edalati, M. Ameri, M. Iranmanesh and Z. Sadeghi, "Solar photovoltaic power plants in five top oil-producing countries in Middle East: A case study in Iran", Renewable and Sustainable Energy Reviews, vol. 69, pp. 1271-1280, 2017. Available: 10.1016/j.rser.2016.12.042.

[17] T. Huld, “PVMAPS: Software tools and data for the estimation of solar radiation and photovoltaic module performance over large geographical areas”. Solar Energy, 142, 171-181, 2017.

[18] M. H. Ahmadi, et al. "Solar power technology for electricity generation: A critical review." Energy Science & Engineering 6.5, pp. 340-361, 2018.

[19] A. Yushchenko, et al. "GIS-based assessment of photovoltaic (PV) and concentrated solar power (CSP) generation potential in West Africa." Renewable and Sustainable Energy Reviews 81, pp. 2088-2103, 2018

[20] P. Blanc, et al. "Direct normal irradiance related definitions and applications: The circumsolar issue." Solar Energy 110, pp. 561-577, 2014.

[21] M. Marzband, et al. "Framework for smart transactive energy in home-microgrids considering coalition formation and demand side management." Sustainable cities and society 40, pp. 136-154, 2018.

[22] P. Alamdari, O. Nematollahi, and A. Alemrajabi. "Solar energy potentials in Iran: A review." Renewable and Sustainable Energy Reviews 21, pp. 778-788, 2013

[23] Available: http://solargis.com/ products/maps-and-gis-data/free/download/iran.

[24] S. Naserpour, H. Zolfaghari, and P. Zeaiean Firouzabadi. "Calibration and evaluation of sunshine-based empirical models for estimating daily solar radiation in Iran." *Sustainable Energy Technologies and Assessments* 42, 2020.

[25] Beopt.nrel.gov. (2017). Home | BEopt. http://BEopt.nrel.gov.

[26] J. Mariola," Optimization of Stand-Alone Hybrid Solar-Wind System by Using General Morphological Analysis. Modeling, Simulation and Optimization of Wind Farms and Hybrid Systems". P.163. 2020

[27] J. F. Manwell, J. G. McGowan and A. L. Rogers, "Wind Energy Explaned Theory, Design and Application Second Edition", pp447-501, 2009.

[28] A. Mohamed. "A finite control set model predictive control scheme for single-phase grid-connected inverters." Renewable and Sustainable Energy Reviews 135 (2021): 110131.

[29] A.Yazdani and R. Iravani, Voltage-Sourced Converters: Modeling, Control, and Applications. Hoboken, NJ: Wiley, 2010.

[30] C. Vargas-Salgado, et al. "Low-cost web-based Supervisory Control and Data Acquisition system for a microgrid testbed: A case study in design and implementation for academic and research applications." Heliyon 5.9, 2019

[31] S. Sahin, M. Ölmez and Y. Isler, "Microcontroller-Based Experimental Setup and Experiments for SCADA Education," IEEE Transactions on Education, vol. 53, no. 3, pp. 437-444, Aug. 2010. doi: 10.1109/TE.2009.2026739

[32] L. Abbey, "Telemetry / SCADA Open Systems vs Proprietary Systems," Available Online: https://www.abbey.co.nz/telemetry–scada-open-vs-proprietarysystems-2003.html

[33] K. Chakraborty, M. G. Choudhury, S. Das, and S. Paul. "Development of PLC-SCADA based control strategy for water storage in a tank for a semi-automated plant." Journal of Instrumentation 15, no. 04, 2020.

[34] S. U. Abdi, K. Iqbal and J. Ahmed, "Development of PC-based SCADA training system," 2016 IEEE International Conference on Industrial Technology (ICIT), Taipei, 2016, pp. 1192-1197. doi: 10.1109/ICIT.2016.7474923

[35] A. Armando, et al. "Synchronizing NTP Referenced SCADA Systems Interconnected by High-availability Networks." 2020 XXXV Conference on Design of Circuits and Integrated Systems (DCIS). IEEE, 2020

[36] T. Turc, A. Gligor and C. D Dumitru, "Web-based Wireless Sensor System for SCADA Environment," Procedia Engineering 181 (2017) 546 – 551. https://doi.org/10.1016/j.proeng.2017.02.432

[37] M. Jafar, "SCADA Control of a Water Pumping Station,". Available Online: https://www.hackster.io/muntadharjafar/scada-control-of-a-water-pumping station f4cdd4.

Chapter 2: Optimal sizing of a PV system in Golpayegan, Iran using thermal modeling-based load demand

This chapter is a paper accepted in European Journal of Engineering Research and Science and authored by Atefeh Zare and Dr. M. Tariq Iqbal and was published on European Journal of Engineering Research and Science (EJERS). The MEng candidate was involved with the planning and calculation of the experiments, method selection, the data analysis, and the writing of the paper.

2.1 Abstract

This paper introduces the design and analysis of a Photovoltaic (PV) system to supply the residential load of a house in Golpayegan, Iran. The paper's procedure is the house's thermal modeling employing BEopt software to estimate the load data and then collect the primary meteorological data such as solar irradiance and temperature for the selected site. After these preliminary steps, system optimization for PV/grid and PV/diesel/battery models are developed using the HOMER software. The optimization found that the PV array required capacities are 5.17 kW and 6.19 kW, producing 9,346 kWh/yr and 11,196 kWh/yr for standalone and grid-connected PV systems, respectively. The results indicate that solar energy utilization is an attractive option for grid-connected and standalone PV

systems, of which the net present costs (NPC) of each system are 12,180 US$, 40,618 US$, respectively. The system analyses show that adopting either a PV/grid or PV/diesel/battery system causes a reduction in not only dependency on fossil fuel but also in CO2 emission.

2.2 Introduction

Due to growing attention to climate change, many countries have agreed to reduce carbon emissions based on the Kyoto Protocol. According to the protocol, carbon emissions must be reduced 50% by 2050. Hence, those countries attempt to use environmentally friendly sources. To reduce climate change problems, using renewable energy sources is a feasible and effective solution [1]. The commitment of renewable energy systems (RES) promotes clean electricity [2]. In general, RESs are adopted to supply domestic, manufacturing, and farming loads. When considering new technologies in RESs and the nonstationary characteristics of these RE sources, the optimal supervision and reliable power generation performance from RESs has been more critical in investigations done recently. These investigations examine the benefits and drawbacks of RE sources, the optimization of RESs, environmental pollution mitigation, and enhancement in the system's final cost [3-5].

Due to the high availability of solar energy in most countries, its different applications are widely used throughout the world [6]. As manufacturing the solar photovoltaic (PV) devices at a lower cost becomes a reality, PV systems have been extensively adopted in small-sized applications. They are one of the most promising candidates for investigations and large-scale developments [7].

With an average annual radiation exposure of 4.5 kWh/ m^2/day, Iran has a unique potential for using PV systems [8]. Haratian et al. [9] proposed a RES including PV/wind/batteries for a standalone power generation in Iran; they employed HOMER software to detect the best RES configuration considering an estimated power consumption. Among different RESs configuration, one which was economically the best was the combination of photovoltaic panel and batteries, with a total NPC of 8173 US. Elsewhere Jahangir et al. in [10] presented a hybrid organic Rankine cycle for a domestic location in Rayen, Iran. HOMER software was used to model RES. The results showed that the optimal power system was a hybrid system consists of PV/ wind/diesel/battery with NPC of 268,592 $. Shirinabadi et al. [11] proposed a grid-connected solar system in Tabriz, Iran, as an agricultural application of solar systems. Simulations showed that 20.164% of the required energy of selected site was provided by the solar system and 79.836% supplied by the utility grid. The proposed system decreased the carbon emission by about 508713.5232 kg annually. Shahinzadeh et al. [12] Proposed RES included wind/PV/microturbine/battery /fuel cell and utilized HOMER software to estimate the size of power generation units in a grid-connected RES located in Nain, Iran.

Optimal planning principally aims to achieve the best RES combination based on the lowest NPC ($/kWh), COE (%), and carbon emission for both grid-connected and standalone power generation systems [9].

In this paper, RE solutions for both standalone and grid-connected power generation for a household in Golpayegan, Iran, are provided to meet the load demand of the selected place. The chosen house's thermal modeling is carried out using BEopt software to estimate the

house's power consumption. The most cost-effective system's design has been carried out adopting HOMER Pro based on the estimated load power consumption and technical and economic parameters of power generation components. The load following (LF) dispatch strategy is used to control the systems.

2.3 Methodology

To successfully evaluate any renewable energy system, employing appropriate criteria in the chosen site, it is necessary to make sure that the operational performance of various designs is precisely examined. The following examination frameworks have been selected in this paper:

- Specifications of selected location and load demand data
- Metrological data
- System components
- Mathematical description
- Operational control of the system

2.3.1 Specification and Load Profile of the Selected Site

When designing a RES for a house, it is essential to determine the house energy demands accurately. The thermal modeling of a home is used to achieve this goal [13,14]. As a case study, the selected house is in Golpayegan, Isfahan Province, Iran (33°27'20.5"N 50°16'58.3"E). Thermal modeling is completed with residential load estimation using

BEopt software to estimate the house's power consumption based on the meteorological data, specification of the house, and the power consumption of typical appliances used by residents.

Since there are substantial natural oil and gas sources in Iran, people do not use electricity for cooking and heating purposes. Thus, the typical load demand is not significant. According to the BEopt results, the house requires an annual energy consumption of 11222 kWh/year (about 30.74kWh/day average load), as shown in Fig. 3. The monthly and daily load profile and their average for a year were generated and displayed in Fig. 4, which confirms that the load demand is quietly greater in May, June, July, August, and September due to hot temperature use of air conditioner.

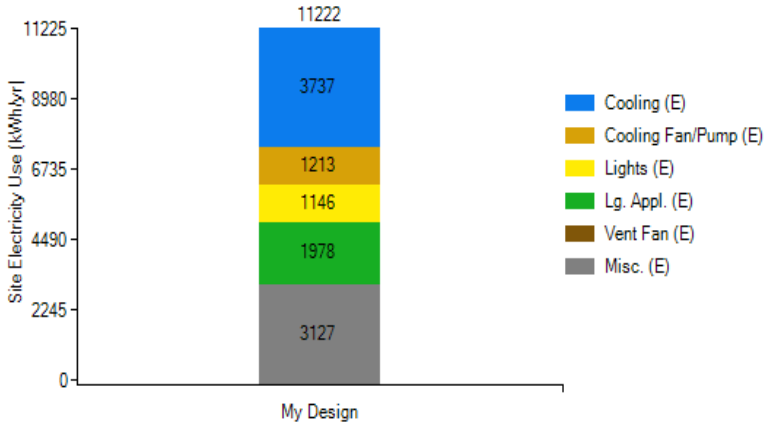

Fig. 3-Annual energy consumption of the house based on BEopt modeling.

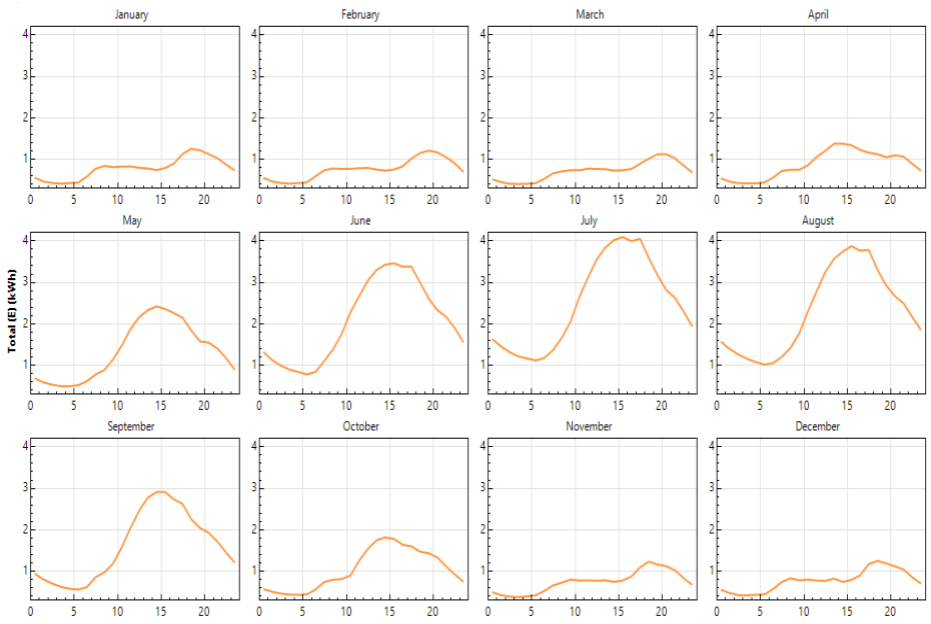

(a)

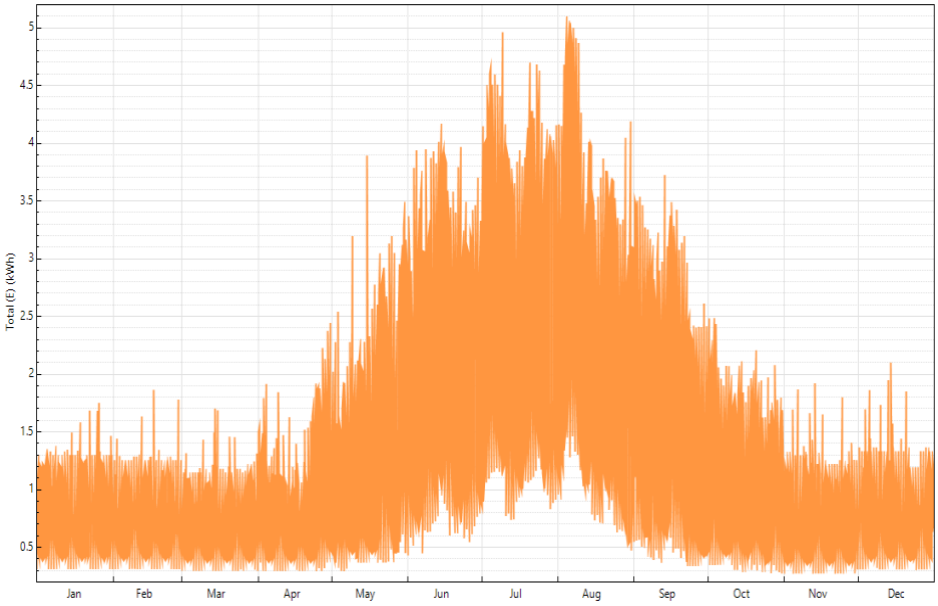

(b)

Fig. 4- (a) Monthly and (b) Daily load of the residence during a year.

2.3.2 The Metrological data

Solar radiation and ambient temperature significantly impact the PV output power. The following points describe solar irradiance and temperature at the selected city, obtained from National Aeronautics and Space Administration (NASA) website.

2.3.2.1 Solar radiation

Fig. 5 presents the solar irradiance and clearance index data for the decided residence. The annual average and the maximum value of solar irradiance are 5.15 kWh/m2/day and 7.61 kWh/m2/day, respectively. Golpayegan city receives a noticeable volume of solar irradiance which confirms that solar power plant is a significant energy source.

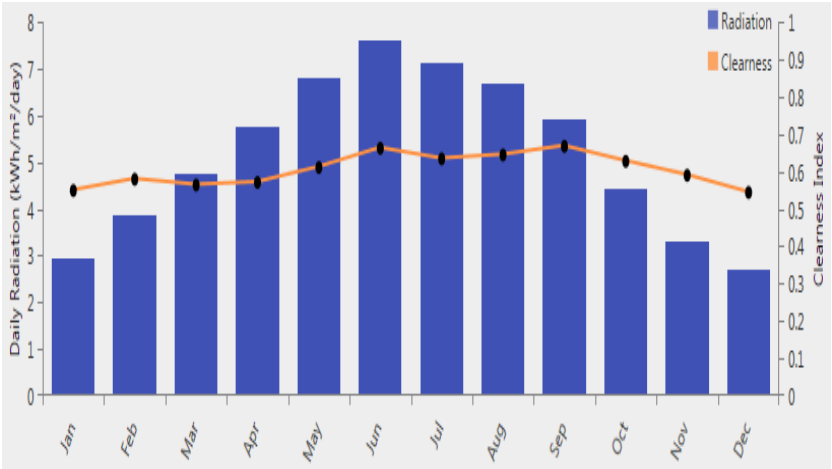

Fig. 5-Monthly solar and clearance index of the selected site.

2.3.2.2 Ambient temperature

Ambient temperature plays an essential role in the PV panels' performance. Hence, a correct evaluation of ambient temperature data is crucially important. As Fig. 6 demonstrates, the selected site's ambient temperature, summer has the most significant ambient temperature in July at 24.31 °C, and the lowest ambient temperature is in January at -1.76 °C.

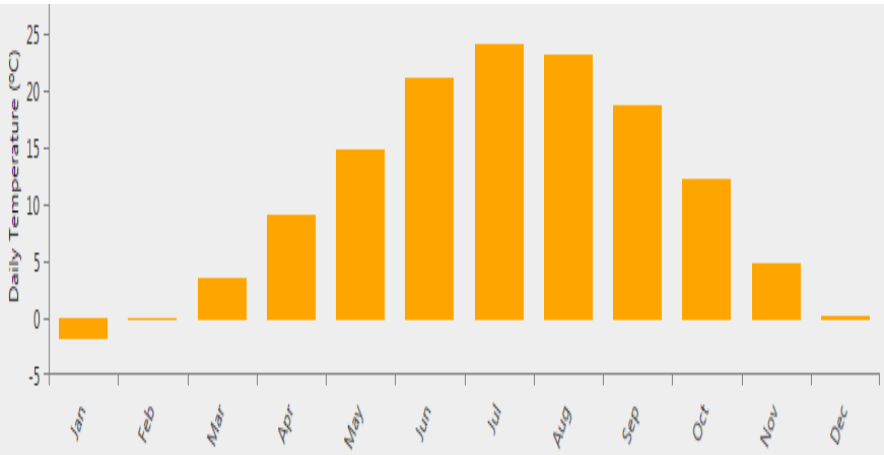

Fig. 6-Monthly temperature of the selected site.

2.3.3 Power System Components

In this investigation, two RESs are proposed and investigated. They are then economically compared to each other to find out the best one for the selected site. The first one is a grid-connected RES, consisting of three components: the PV panels, converter, and grid. The second one is a stand-alone RES that comprises four parts: the PV panels, diesel generator, inverter, and some batteries. Schematic diagrams of the purposed RESs are depicted in Fig.

7. The techno-economic information of components for both configurations are defined in specification in Table 1. Imported load data into HOMER software is shown in Fig. 8.

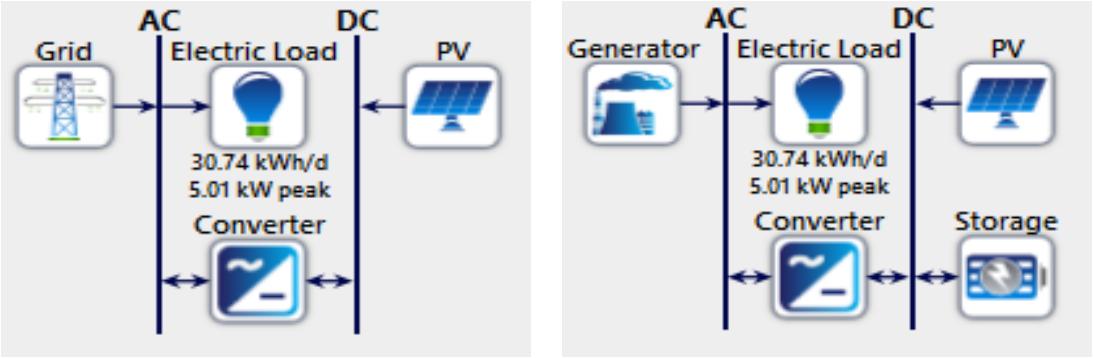

(a) *(b)*

Fig. 7-Grid-connected PV system (b) Standalone PV system.

Table 1 Input Parameters and Costs of Different Components

Component	**Cost**			**Other information**
	Capital ($/kW)	***O&M ($/kW)***	***Replacement ($/kW)***	
PV panel	1500	10 (1/year)	1125	Tracking system: fixed Temperature coefficient = -0.39%/° C Efficiency = 17.72% derating factor = 90% Nominal operating cell temperature = 45°C Lifetime: 25 years
Converter	350	10 (1/year)	300	Efficiency = 97% Lifetime: 10 years
Generator	220	0.03(1/h)	200	Lifetime: 15000 h
Battery	130	1 (1/year)	100	Nominal capacity: 200Ah Nominal voltage: 1.2V

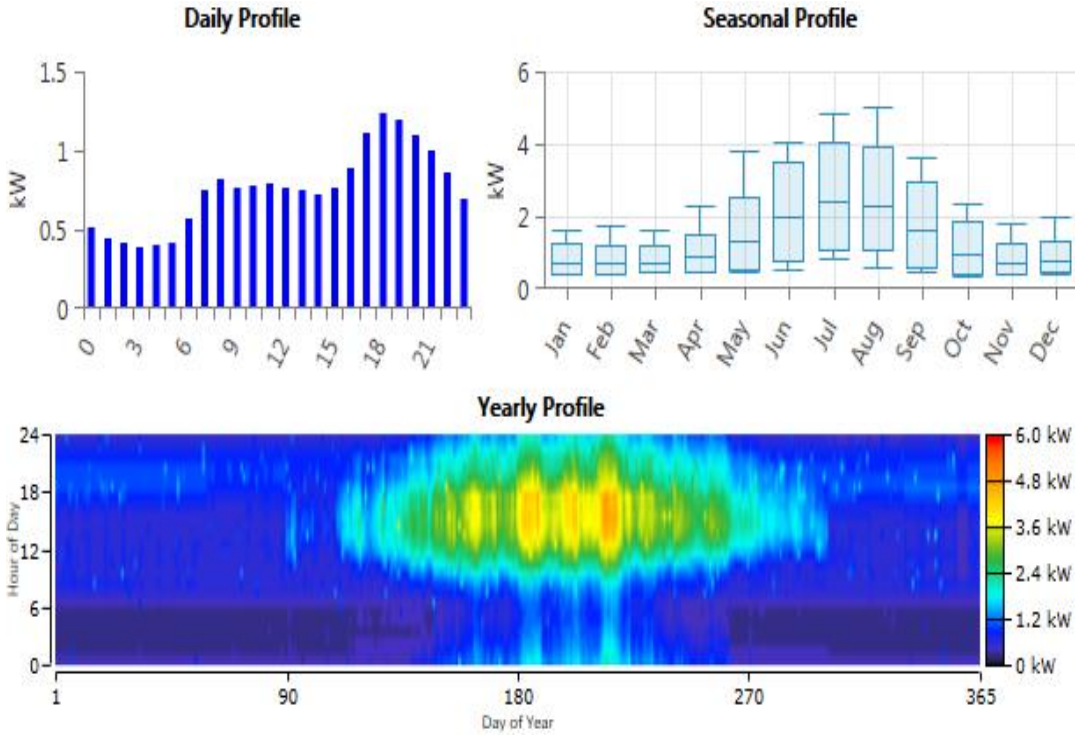

Fig. 8-load profile data into HOMER.

2.3.4 Mathematical Representation

2.3.4.1 PV Output Power

The available solar irradiance and temperature considerably influence the output power of PV. The following equation is adopted in HOMER to calculate the PV generated power based on the input parameters [15]:

$$P_{PV}(i, t) = Y_{PV} * f_{PV} (G_T/G_{T,STC})[1+a_p (T_c - T_{c,STC})) \qquad (1.2)$$

STC depicts the standard test conditions. Y_{PV} and f_{PV} refer to the PV rated capacity under STCs and derating factor. G_T and $G_{T,STC}$ express incident irradiance on the PV panel at the moment and under STCs, respectively. The coefficient of temperature is represented by α_P. T_c and $T_{c,STC}$ are the PV cell temperature (˚C) at the moment and under STCs (25 ˚C), respectively.

2.3.4.2 Economic Design

Supposing that HOMER software intends to lessen system operating costs and discover the optimal system configuration, economics plays an essential role in related simulations. The optimal combination of RES components is achieved based on the lowest NPC. NPC is a combination of revenues and all expenses over the project lifetime. considering the following equation, the system NPC is obtained as follows [16]:

$$NPC = (C_{ann,tot} / CRF(i, T_p)) \qquad (2.2)$$

$C_{ann,tot}$ represents the total annualized cost ($/year). i refers to the annual interest rate (%), T_p is the endurance of the designed system (year), and CRF indicates the capital recovery factor, which is obtained by [16]:

$$CRF\ (i, n) = ([i(1+i)^{n}] / [(1+i)^{n}-1]) \qquad (3.2)$$

In equation (3) n is the number of years. The components' residual values are considered toward the NPC calculation. It is known as salvage costs (SC), which can be obtained using the following equation:

$$SC = C_{RC}\,(T_{rem} / T_{com}) \qquad (4.2)$$

C_{RC} implies the cost of replacement ($). T_{rem} is considered as the remained lifetime of components, and T_{com} indicates the component lifetime.

the cost of energy has been shown by COE which is obtained by following expression [14]:

$$COE = C_{ann,tot} / E_{ann,tot} \qquad (5.2)$$

$E_{ann,tot}$ presents the total served electrical load (kWh/year).

2.3.5 Control Strategy

In this paper, the load following (LF) strategy is presented as a RES controller. The system operation of this controller follows three principles [14]:

1. When the PV output power and load demand are equal, the output power of PV array fulfills the power consumption of the load, so there is no excess power.
2. When the PV generated power is greater than the power consumption of the load, therefore:

- In PV/grid configuration, the excess energy is injected into the grid.
- In PV/diesel/battery configuration, if the battery is fully charged, the excess power is damped. However, the extra power of PV charges the battery if it is not fully charged. In this case, the generator also does not start working.

3. The PV generated power is less than the load required energy; thus:

- In PV/grid, the required energy will be provided by the grid.
- In PV/diesel/battery design, two potential conditions are presents as follows:
    - If SOC = SOC_{min}, the gross load demand (P_L-P_{PV}) is provided by the generator with no battery charging. If the minimum generated power of generator is greater than the needed gross power demand of the load, then the net load demand is supplied by the generator, while PV charges the battery.
    - If SOC> SOC_{min}, HOMER calculates the battery discharging cost and compares it to the cost of turning the generator on. If the discharging cost of the storage is less than the cost of turning on the generator, the storage will be discharged to meet the load demand. Otherwise, the generator will be run to fulfill the load required energy.

2.4 Results and Discussion

The technical feasibility is investigated to examine the available power's capability to meet the load demand for a year. Then, HOMER software examines the economic sustainability and environmental consequences of the suggested systems. The uncertain specifications of the power system are shown in table 2.

The feasible systems can satisfy the load demands and are presented by their NPC in HOMER software. The best optimal combination of RES for PV/grid and PV/diesel/battery systems are provided in Tables 3 and 4. The electric production for both RES systems is illustrated in Fig. 9 and 10 based on the months.

Table 2 Optimization results of the PV/grid RES

Item	Unit	Value
PV	kW	6.19
Converter	kW	5.03
NPC	$	12,180
COE	$/kWh	0.056
Renewable fraction	%	64.1
PV production	kWh/year	11,196
Grid purchases	kWh/year	5976
Total production	kWh/year	17,172
Excess energy	%	0.5
Carbon emission	kg/year	3,777
Capital cost	$	5,349.48
O&M cost	$	5,679.5
Replacement cost	$	1,332.5

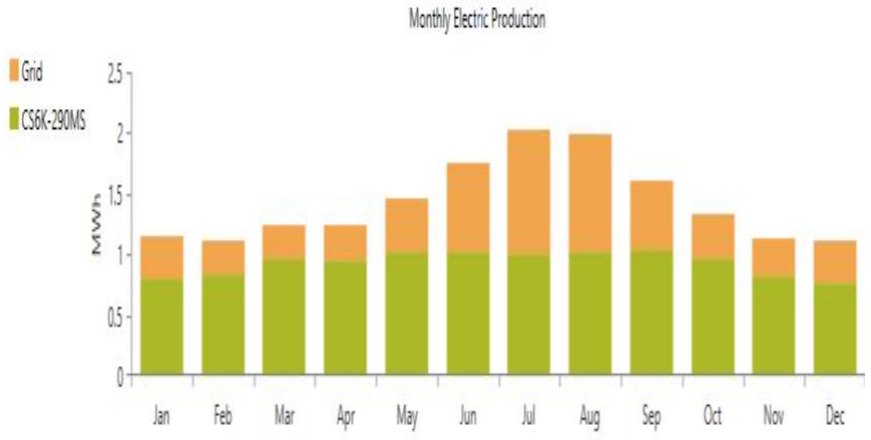

Fig. 9-Monthly average electric production for Grid-connected PV system.

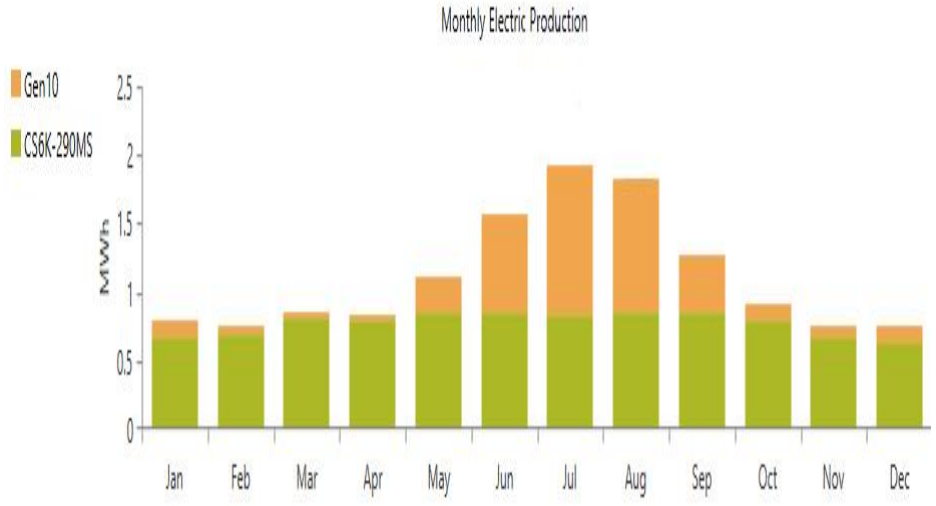

Fig. 10-Monthly average electric production for standalone PV system.

when the storage supplies the load but does not get charged in the primary breakdown. Reaching some BT is essential, mainly when the PV generated power cannot satisfy the load requirement [17]. The BT is 12.1 h for PV/grid/batteries configuration based on the simulation results in this investigation.

Table 3 Optimization results of the PV/diesel/ battery RES.

Item	Unit	Value
PV	kW	5.17
Battery	Strings	36
Diesel generator	kW	10
Converter	kW	6.67
NPC	$	40.618
COE	$/kWh	0.28
Renewable fraction	%	64.2
PV production	kWh/year	9,346
Grid purchases	kWh/year	4,019
Total production	kWh/year	13,365
Excess energy	%	8
Carbon emission	kg/year	4,969
Capital cost	$	12,210
O&M cost	$	2,811
Replacement cost	$	1,827
Salvage cost	$	-819
Battery autonomy	hr	12.1
Fuel consumption	L/year	1902

2.5 Conclusions

In this work, the evaluation of RES is technically and economically performed to provide the selected household with power in Golpayegan, Iran. First, the thermal modeling of the chosen house is carried out by using BEopt software. The RES configurations are

suggested, which include PV/grid and PV/diesel/battery. HOMER software adopted to simulate and model these configurations. LF control strategy is adopted in this study to manage the power generation. The cost investigation shows that the PV/grid has a PV array of 6.19 kW and an inverter of 5.03 kW, and its NPC is $12,180 and a COE of 0.056 $/kWh. However, the optimal solution of PV/diesel/battery configuration consists of a PV array of 5.17 kW, a diesel generator of 10kW, 36 storage, and an inverter of 6.67 kW. Its net present cost is $40,617, and the cost of energy is 0.28 $/kWh, which is more expensive than the PV/grid system.

References

[1] H. Rezzouk and A. Mellit, "Feasibility study and sensitivity analysis of a standalone photovoltaic–diesel–battery hybrid energy system in the north of Algeria", Renewable and Sustainable Energy Reviews, vol. 43, pp. 1134-1150, 2015.

[2] A. Fathima and K. Palanisamy, "Optimization in microgrids with hybrid energy systems – A review", Renewable and Sustainable Energy Reviews, vol. 45, pp. 431-446, 2015.

[3] L. Meng, E. Sanseverino, A. Luna, T. Dragicevic, J. Vasquez and J. Guerrero, "Microgrid supervisory controllers and energy management systems: A literature review", Renewable and Sustainable Energy Reviews, vol. 60, pp. 1263-1273, 2016.

[4] R. Kamel, "New inverter control for balancing standalone micro-grid phase voltages: A review on MG power quality improvement", Renewable and Sustainable Energy Reviews, vol. 63, pp. 520-532, 2016.

[5] Z. Shuai, Y. Sun, J. Shen, W. Tian, C. Tu, Y. Li, and X. Yin, "Microgrid stability: Classification and a review", Renewable and Sustainable Energy Reviews, vol. 58, pp. 167-179, 2016.

[6] M. Esen and T. Yuksel, "Experimental evaluation of using various renewable energy sources for heating a greenhouse", Energy and Buildings, vol. 65, pp. 340-351, 2013.

[7] A. Shiroudi, S. Taklimi, S. Mousavifar and P. Taghipour, "Standalone PV-hydrogen energy system in Taleghan-Iran using HOMER software: optimization and techno-economic analysis", Environment, Development and Sustainability, vol. 15, no. 5, pp. 1389-1402, 2013.

[8] G. Najafi a,n, B.Ghobadian a, R.Mamat b, T.Yusaf c, W.H.Azmi b “Solar energy in Iran: Current state and outlook”, Renewable and Sustainable Energy, vol. 49, pp. 931-942, 2015.

[9] M. Haratian, P. Tabibi, M. Sadeghi, B. Vaseghi and A. Poustdouz, "A renewable energy solution for standalone power generation: A case study of KhshU Site-Iran", Renewable Energy, vol. 125, pp. 926-935, 2018.

[10] M. Jahangir, S. Mousavi and M. Vaziri Rad, "A techno-economic comparison of a photovoltaic/thermal organic Rankine cycle with several renewable hybrid systems for a residential area in Rayen, Iran", Energy Conversion and Management, vol. 195, pp. 244-261, 2019.

[11] M. Shirinabadi and A. Azami, "The Feasibility of Photovoltaic and Grid-Hybrid Power Plant for Water Pumping Station in Tabriz-Iran," 2018 International Conference on Photovoltaic Science and Technologies (PVCon), Ankara, pp. 1-4, 2018.

[12] H. Shahinzadeh, M. Moazzami, S. H. Fathi and G. B. Gharehpetian, "Optimal sizing and energy management of a grid-connected microgrid using HOMER software," 2016 Smart Grids Conference (SGC), Kerman, pp. 1-6, 2016.

[13] A. Iqbal and M. Iqbal, "Design and Analysis of a Standalone PV System for a Rural House in Pakistan", International Journal of Photoenergy, vol. 2019, pp. 1-8, 2019.

[14] L. Aghenta and M. Iqbal, "Design and Dynamic Modelling of a Hybrid Power System for a House in Nigeria", International Journal of Photoenergy, vol. 2019, pp. 1-13, 2019.

[15] A. Aziz, M. Tajuddin, M. Adzman, M. Ramli and S. Mekhilef, "Energy Management and Optimization of a PV/Diesel/Battery Hybrid Energy System Using a Combined Dispatch Strategy", Sustainability, vol. 11, no. 3, p. 683, 2019.

[16] Y. Alharthi, M. Siddiki and G. Chaudhry, "Resource Assessment and Techno-Economic Analysis of a Grid-Connected Solar PV-Wind Hybrid System for Different Locations in Saudi Arabia", Sustainability, vol. 10, no. 10, p. 3690, 2018.

[17] K. Tharani and R. Dahiya, "Choice of battery energy storage for a hybrid renewable energy system", TURKISH JOURNAL OF ELECTRICAL ENGINEERING & COMPUTER SCIENCES, vol. 26, no. 2, pp. 666-676, 2018.

Chapter 3: Dynamic Modeling and Control of a Single-Phase Grid-Connected photovoltaic System

This chapter is a paper accepted in European Journal of Electrical Engineering and Computer Science and authored by Atefeh Zare and Dr. M. Tariq Iqbal and was published on European Journal of Engineering Research and Science (EJECE). The MEng candidate was involved with the planning and calculation of the experiments, method selection, the data analysis, and the writing of the paper.

3.1 Abstract

Designing control strategies to connect a photovoltaic (PV) system to the grid has been significantly challenging. This paper focuses on developing a controller for a single-phase PV system connected to the grid and its implementation to modify the power factor in the distribution power system. To design a grid-connected PV system, its components are modeled, such as PV panels, Maximum Power Point tracking (MPPT) algorithm, the grid interface inverter with the appropriate filter, and the DC link capacitor. SIMULINK / MATLAB is used for simulation in this study. The proposed control strategy is designed

to track the maximum power point of The PV panels and control the PV active and reactive output power. In this paper, the presented reactive power control provides the PV system with power factor correction (PFC) capability. The proposed technique for checking controller validity is tested, and the results prove that the proposed controller is good and provides the required performance.

3.2 Introduction

Fossil fuels significantly satisfy global energy demand and are likely to keep their future impact. However, fossil fuel sources are limited, so that they cannot meet worldwide energy demands. Therefore, renewable energy sources (RES) importance has been evident. Solar energy systems are one of the most widely utilized sources of RESs [1]. Another advantage of using solar energy is that in contrast with fossil fuel power plants, the sun's energy has no adverse impact on the environment [2,3]. Hence, researchers pay more attention to this issue. PV systems are widely utilized in various fields, such as grid-connected systems, heating and irrigation applications, and space transportation. Energy production takes many advantages of PV panels [4]. However, performance depends on meteorological conditions such as temperature, solar radiation level, shading, and dust.

Therefore, transferring the maximum power from PV panels is a significant concern. By employing a power point tracking technique, the highest available amount of energy is captured. The most common MPPT techniques are Perturb & Observe and Incremental Conductance algorithms because they are simple and highly effective [5]. Since these

techniques are autonomous of photovoltaic characteristics while tracking the Maximum Power Point (MPP), they are the most advantageous techniques.

As a result, MPPs accomplishments attract more attention, which are essential circumstances for inverter tied to the grid controlling active (P) and reactive (Q) power [6]. Several researchers have investigated grid-connected inverters. While in some of their research, inverters are suggested to control only the injected P to the grid. Some researchers also investigate multi-functional grid-connected inverters [7,8]. The inverters function to Provide the available PMAX and QMAX, provide Q concerning the voltage, and determine the power factor and reactive power mode [9]. As increasing attention turns to RES, the inverters tied to the grid have received significant attention [10].

In this paper, a control scheme for a single-phase PV system connected to the grid is presented to modify the power factor to prevent grid voltage instability at the Point of Common Coupling (PCC). The incremental conductance method, as an MPPT algorithm, assures the maximum power transfer to the grid. In the proposed system, a single-phase inverter controls the current injected into the grid. The controller adjusts the current without surpassing line restrictions. Moreover, the inverter injects Q required by the grid. The Q demanded by the grid is supported by the PV even when solar irradiation is zero. The control algorithm is simulated, and the evaluation of the results has been done. The suggested control algorithm presented in the study combines the MPPT, P control technique, and power factor controller. Therefore, an effective controller is obtained to directly control the P and Q of the grid-tied PV system.

3.3 Grid Connected Rooftop Photovoltaic System

The schematic diagram of a PV system tied to the grid is presented in Fig. 11. The PV module and the DC-link capacitor are interfaced with the grid via inverter with the proper filter and controllers at PCC.

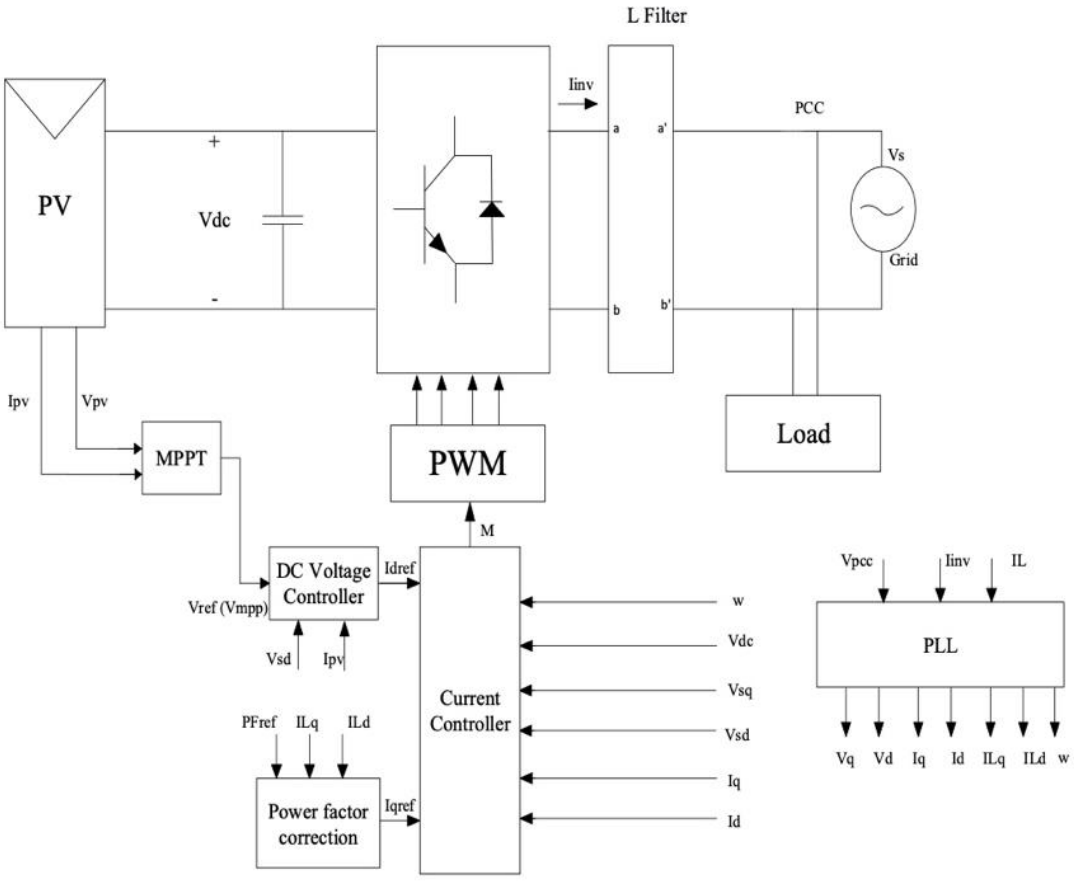

Fig. 11-PV Grid-Tied system block diagram.

I_{inv} and I_L express the inverter output and the load current, respectively. V_s is the source voltage at PCC. The inverter DC link voltage is represented with V_{DC} given by the PV solar system. L_f and C_{DC} refer to the L filter parameter and the DC link capacitor, respectively.

The control strategy suggested in this paper utilizes grid parameters to generate the inverter's control pulses.

3.3.1 PV Source Model

To analyze the grid-connected PV system, modeling the PV module using data from the manufacturer datasheet is essential. Fig. 12 demonstrates the equivalent circuit of a practical PV cell.

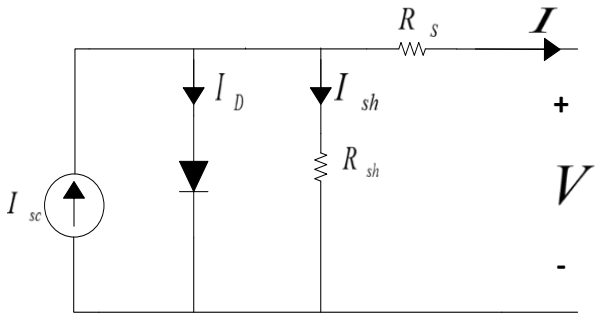

Fig. 12-PV cell equivalent circuit.

It includes a diode non-parallel with a current source, a parallel and a series resistor. The basic equation for describing the I-V properties of a solar cell can be obtained using Kirchhoff's current law on the equivalent circuit of a PV cell.

$$\mathrm{I} = I_{sc} - I_d - I_{sh} \tag{1.3}$$

I, I_{sc}, I_d, and $\mathrm{I_{sh}}$ represent output cell current, short circuit current, the diode current, and the parallel branch current, respectively.

$$I_d = I_o \left[\exp\left(\frac{V - IR_{sr}}{\mathrm{n}kT_c/q}\right) - 1\right] \tag{2.3}$$

$$I_{sh} = (V + IR_{sr})/R_{sh} \tag{3.3}$$

After Substituting the equations (2) and (3) in (1), output cell current has the following equation [15].

$$I = I_{sh} - I_o \left[\exp\left(\frac{V - IR_{sr}}{\mathrm{n}kT_c/q}\right) - 1\right] - \left(\frac{V + IR_{sr}}{R_{sh}}\right) \tag{4.3}$$

$$I_{sc} = I_{scR} \frac{G}{G_R} [1 + \alpha_T (T_c - T_{cR})] \tag{5.3}$$

G refers to solar radiation in the solar cell plate and T_c represents cell temperature. I_o in equation (4) depends on the temperature of the cell. It is called the dark current.

$$I_o = I_{oR}\left(\frac{T_c^3}{T_{cR}^3}\right) exp\left[\left(\frac{1}{T_{cR}}\right) - \frac{1}{T_c}\right]\frac{qe_g}{nk} \tag{6.3}$$

I_{scR} refers to the short-circuit current solar radiation reference G_R and cell temperature reference. α_T represents the temperature coefficient of the photocurrent. I_{oR}, q, and k represent the dark current at T_{cR}, the electron charge, and the Boltzmann constant. e_g and n refer to the solar cell material bandgap energy and the ideality factor of diode.

3.3.2 DC Link Capacitor and L Filter

DC link capacitor is one of the most critical parts of the system as it provides several functions. It minimizes the voltage ripple across the PV terminals, which reduces the output power ripple during the transient states. It acts as a small energy storage unit for providing real power temporarily. Its size is determined as follows [11].

$$C_{dc} = \frac{2P_{max}(\alpha_{max}-1)}{f(V_{dc,high}^2 - V_{dc,low}^2)} \tag{7.3}$$

P_{max} represents the maximum PV output power. f and V_{dc} refer to the frequency and DC-link voltage. α_{max} indicates the ac mains cycle that the DC-side voltage will remain inside its hysteresis band, with $V_{dc,high}$ and $V_{dc,low}$. α_{max} is given as:

$$\alpha_{max} = Round(1 + \frac{V_{dc,high}^2 - V_{dc,low}^2}{V_{dc}^2 - V_{dc,high}^2}) \quad (8.3)$$

For the model used in this paper, $V_{dc,high}$ and $V_{dc,low}$ are 1.15 V_{DC} and 0.8 V_{DC} ,respectively, $P_{max} \approx$ 5 kW, f = 50 Hz, V_{DC} = 500 V.

The higher order harmonics caused by switching the inverter is limited by using an L filter. The value of the L filter of system at the grid side is obtained as follows:

$$L_f = \Delta r \left(\frac{V_{pcc}}{2\pi f I_{inv}}\right) \quad (9.3)$$

Where Δr is the ripple of the current in ac side which considered as %10.

3.3.3 The Inverter Controller Model

The DC-AC inverter performs the conversion of the photovoltaic system direct power to the AC power. The switch-mode inverter produces a sinusoidal AC output from a DC input through PWM [14]. The inverter is a Voltage Source Converter (VSC), in which the

controller works in PFC mode or voltage regulation mode. During PFC mode, the PV exchanges reactive power (Q) for the grid and injects its available active power (P) into the grid. In contrast, in the voltage regulation mode, the PV only generates its available maximum real power. The different subsystems of the PV controller are explained as follows.

3.3.3.1 MPPT Controller

The current and voltage of the photovoltaic cell are related nonlinearly as shown in Fig. 13. At MPP the PV generates its maximum output power. To determine the location of the MPP, several calculation models or search algorithms are developed to keep the PV array performing at its MPP.

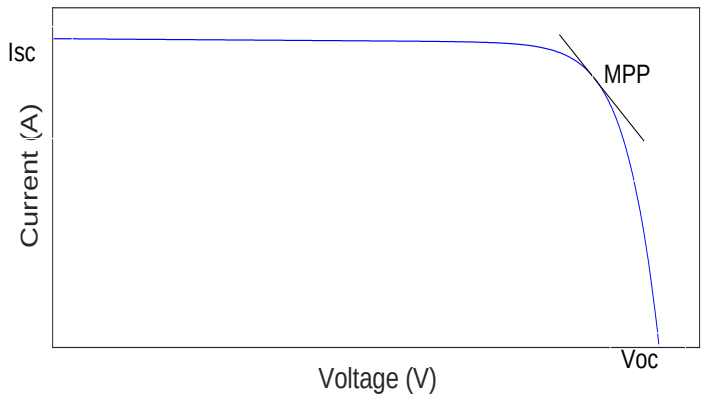

Fig. 13- I/V Characteristics of a PV Cell.

In this paper, the incremental conductance technique is used to find the MPP. Fig. 14 shows the flow chart in which the incremental algorithm detailed operation is described [12]. In this algorithm, the derivative of the output power of the PV array to its output voltage is calculated ($M= dP/dV$). If M is zero, the maximum PV output power is accomplished. If M does not approach zero, the MPPT technique adjusts the PV voltage gradually until M gets close to zero, then the photovoltaic panels move toward its highest output.

3.3.3.2 DC Bus Voltage Control

Fig. 15 presents the DC bus voltage controller. A compensator creates the reference active current, I_{dref}, then the voltage at the DC side is controlled to reach its optimum amount. The DC Bus voltage controller parameters are given in table 1.

3.3.3.3 Power factor controller

Power factor correction is presented in Fig. 16. is generated based on, I_{Ld} and I_{Lq}. I_{Ld} and I_{Lq} refer to direct and quadrature axis current parts consumed by load. I_{Lqnew} refers to load reactive component that needs to be drawn by the load from the grid.

3.3.3.4 Current Controller

The current controller unit plays an essential role in the PV controller. It has two controllers that independently control the VSC active and reactive currents (I_d, I_q) to generate the VSC active and reactive voltages (V_{sd}, V_{sq}). I_d and I_q, are measured and injected into the associated controller. Those signals then are compared to I_{dref} and I_{qref} as reference values Then PI controllers receive error signals and generate active and reactive output voltage

signals. The generated voltage signals are added to respective active and reactive grid voltages (V_{sd}, V_{sq}) and coupling elements to generate inverter terminal voltages (V_{td}, V_{tq}). The current controller, shown in Fig. 17.

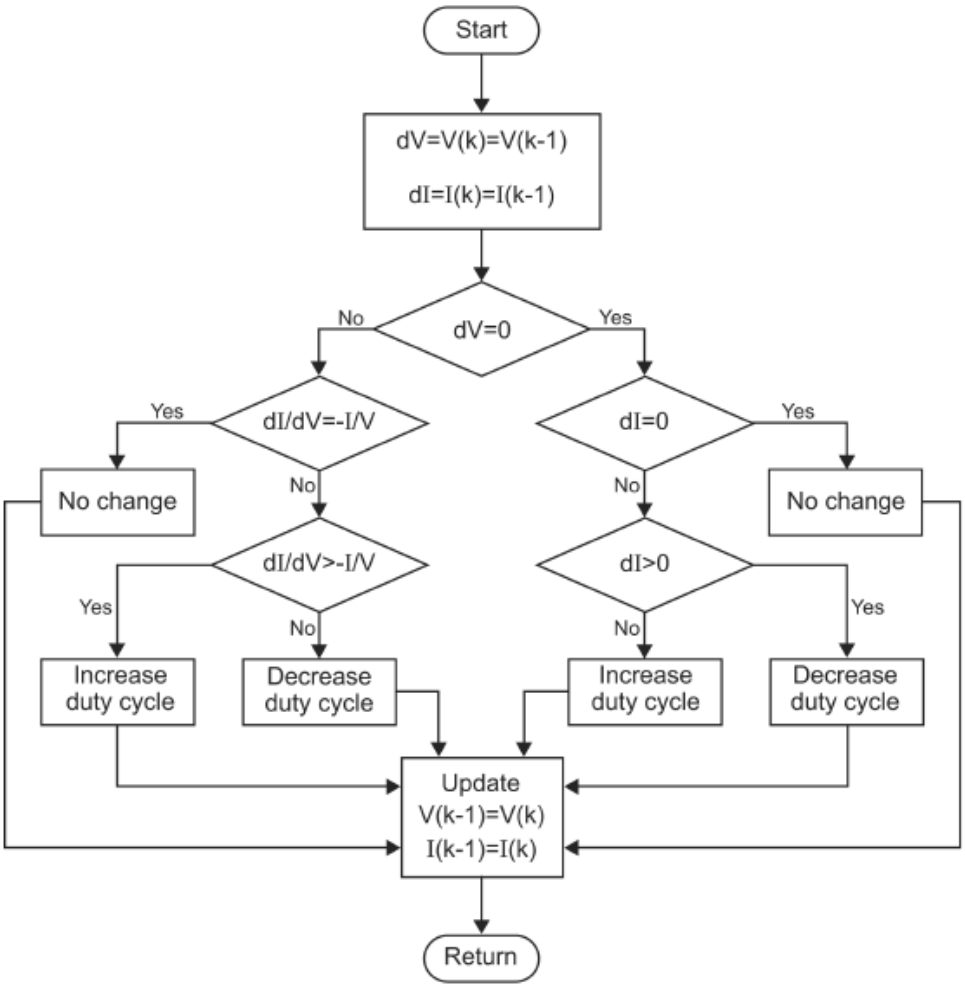

Fig. 14-Flow chart of the incremental conductance MPPT controller [12].

To generate the corresponding components of the modulating signals (M_d, M_q) these VSC terminal voltages are divided by $V_{dc}/2$ [13]. Modulation signals are then transformed into the sinusoidal modulating signal using d-q to abc conversion to generate pulses to switch the inverter. The controller parameters such as K_{pd}, K_{pq}, K_{id}, and K_{iq} are given in table 1.

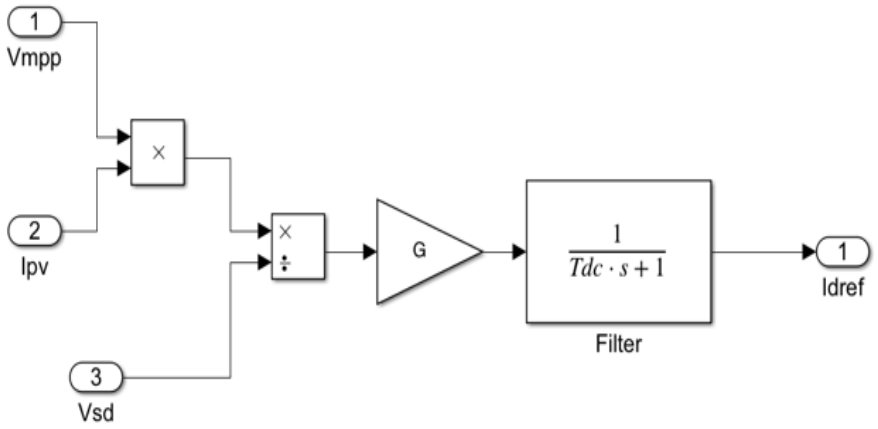

Fig. 15-DC Bus voltage controller.

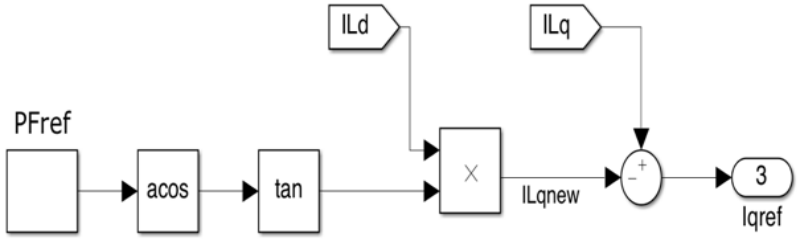

Fig. 16-Power factor controller

3.4 Simulation Results

The implementation of suggested control strategy has been done in the MATLAB/Simulink (R2020a) platform. The system's P, Q, voltage, and current are evaluated through the proposed control technique by considering different solar irradiance. The grid-connected PV system simulation is described in Fig. 18.

The operation of controller is evaluated for 0-0.2s to analyze its performance. Solar radiation levels are changed at t=0.12s and 0.16s to evaluate the results of variation of solar irradiance. The PF correction mode is evaluated during the time 0.035s-0.1s. At t=0.05s, the PV controller operates in power factor correction mode, which causes the source's PF to be one, and PV generates all of the required load reactive power (Q_L). The variation in solar irradiance is tested during the time of $0.1 \leq t \leq 0.2$. At t=0.12s and 0.16s, the PV generation is changed due to variation in solar irradiance.

Table 4 System parameters

System Parameters	Obtained values
Maximum PV power (KW)	5
DC link capacitor (mF)	6.5
Filter inductance (mH)	3.6
Line to line rms voltage (V)	230
AC supply frequency (Hz) 50	50
K_{pd}, K_{pq}	250, 1200
K_{id}, K_{iq}	0.001, 0.9
G, T_{dc}	2, 5e-5

As Fig. 19 shows, the load active (P_L) and Q_L are 3.021 KW and 0.89 kvar, respectively, met by both PV and grid. The grid voltage is 325V, the maximum current, real power (P_S), reactive power (Q_S), and PF of the source are 12.36 A, 1.77 KW, 0.89 kvar, and 0.889, respectively. At the same time, these parameters for inverter output are 7.64 A, 1.256 KW, 0 kvar, and 1. In this simulation time, the PV is working in its unity power factor and generates its maximum available active power capacity in specified solar irradiance and is not injecting any reactive power to the grid.

Fig. 20 demonstrates the PV, load, and source parameters. At 0.05s, the controller starts to operate in PFC mode. When the transient period died out, the P_{PV} is 1.248 kW, and Q_{PV} is 0.89 kvar. Therefore, the controller entirely compensates for the Q_L requirement. Due to the slow DC voltage response, the active power response is slow compared to the reactive power response during the transient period.

Fig. 21 illustrates the evaluation of the proposed controller by changing solar irradiance. As shown in Fig. 21, not only is the power generated by PV follows the rated power, but the power factor correction is also met.

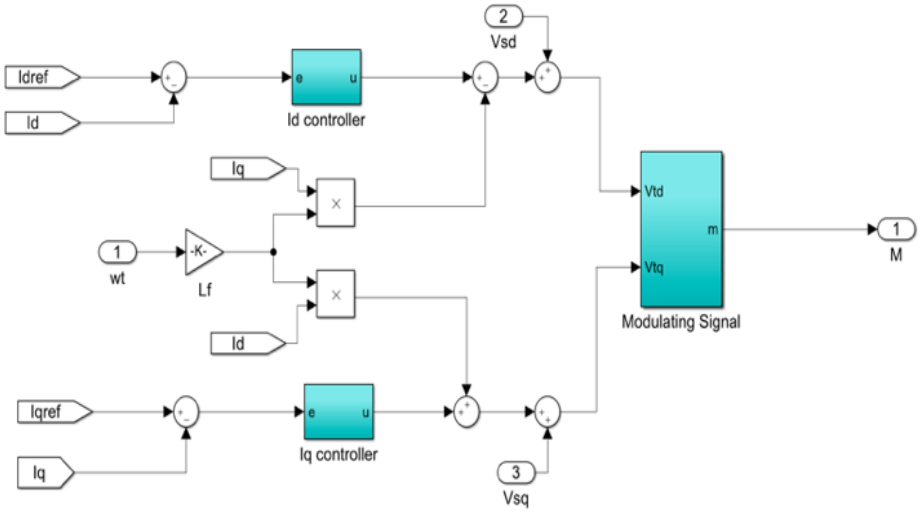

Fig. 17-Current controller.

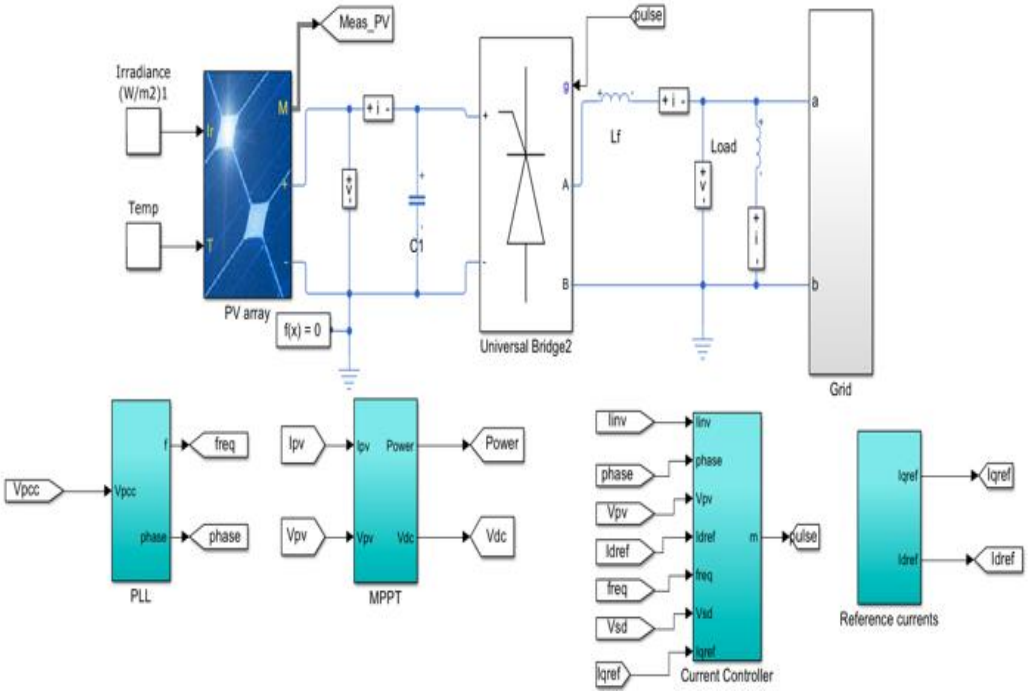

Fig. 18-System simulation.

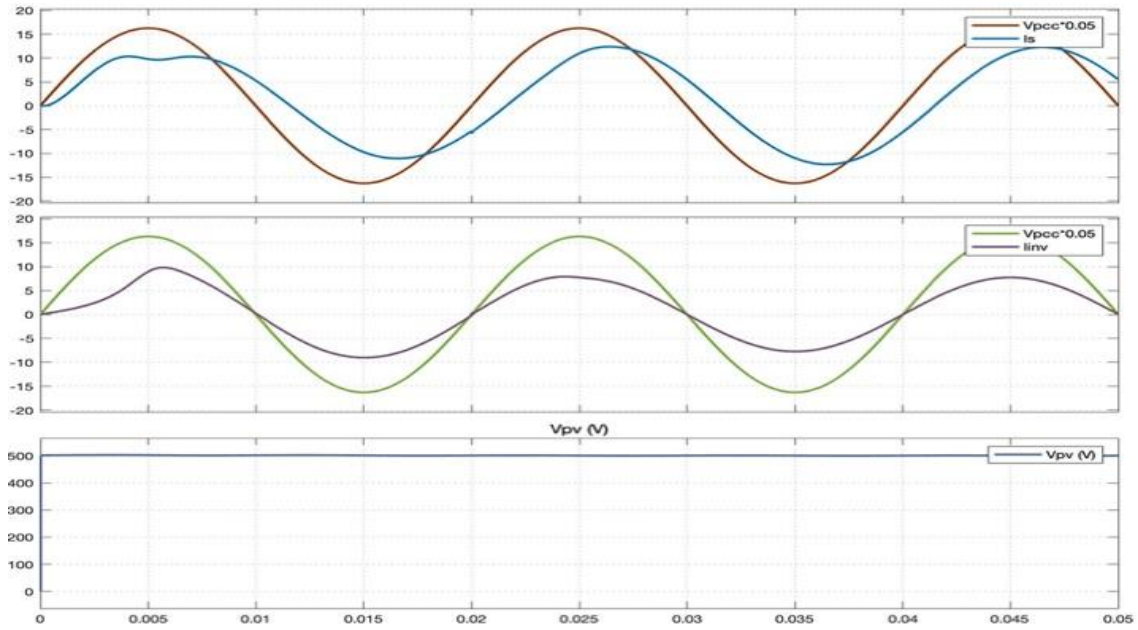

(a)

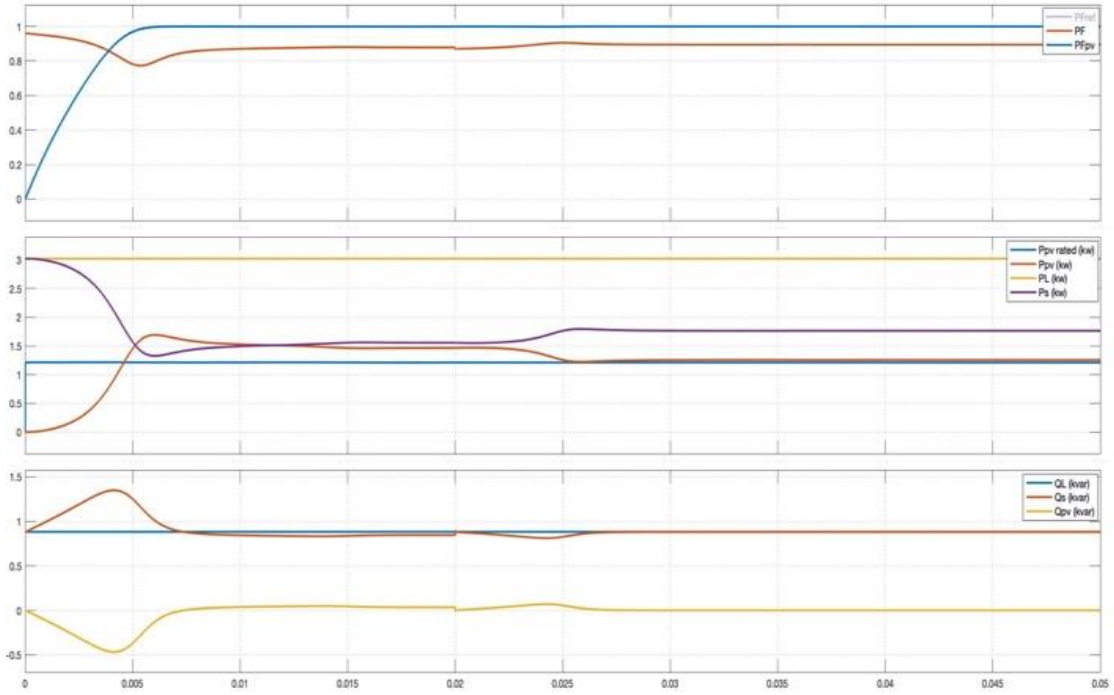

(b)

Fig. 19-(a) Voltage at PCC and DC side- Inverter and Source current. (b) P, Q, and PF of load, inverter, and source.

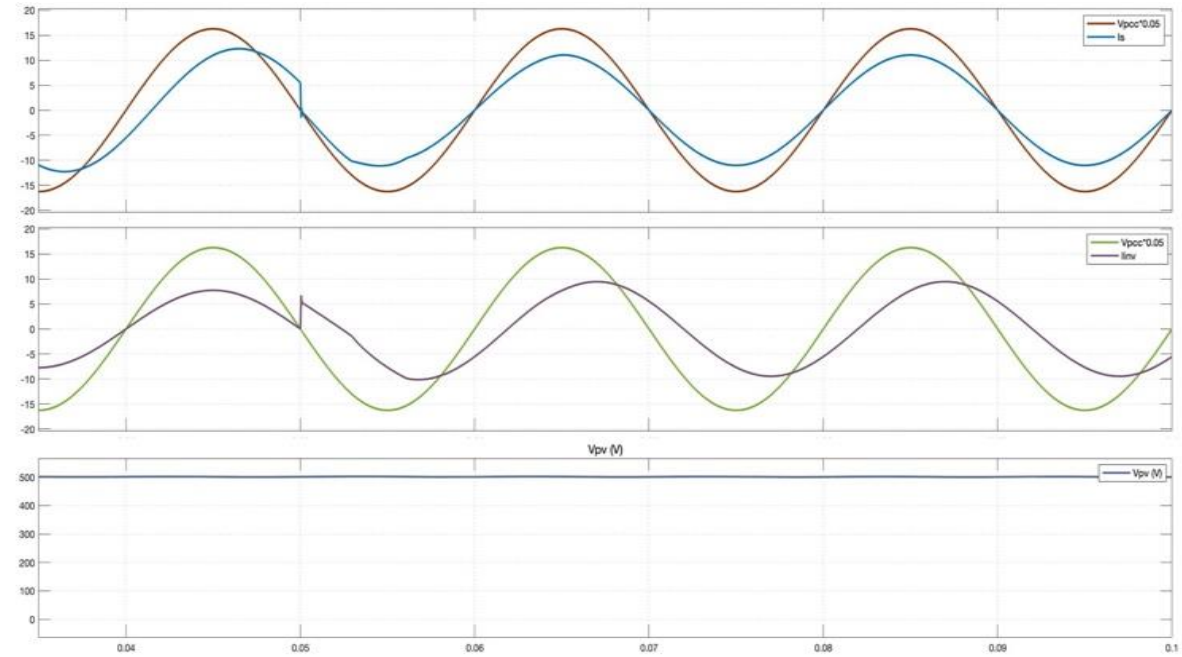

(a)

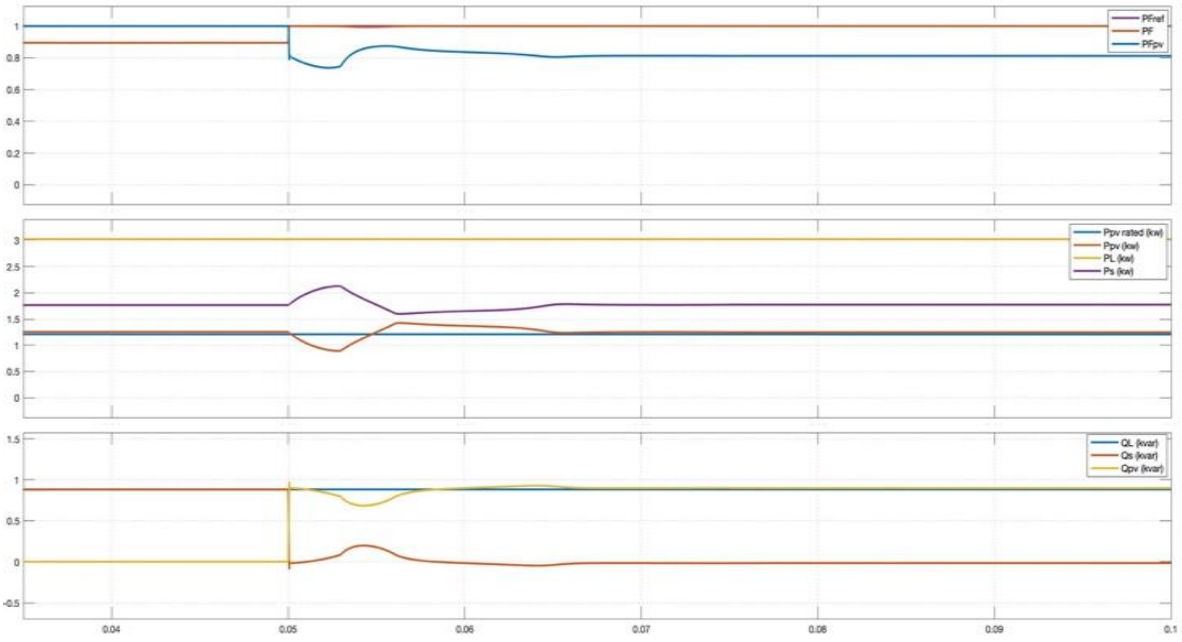

(b)

Fig. 20- (a)Voltage at PCC and DC side- Inverter and Source current. (b) P, Q, and PF of load, inverter, and source.

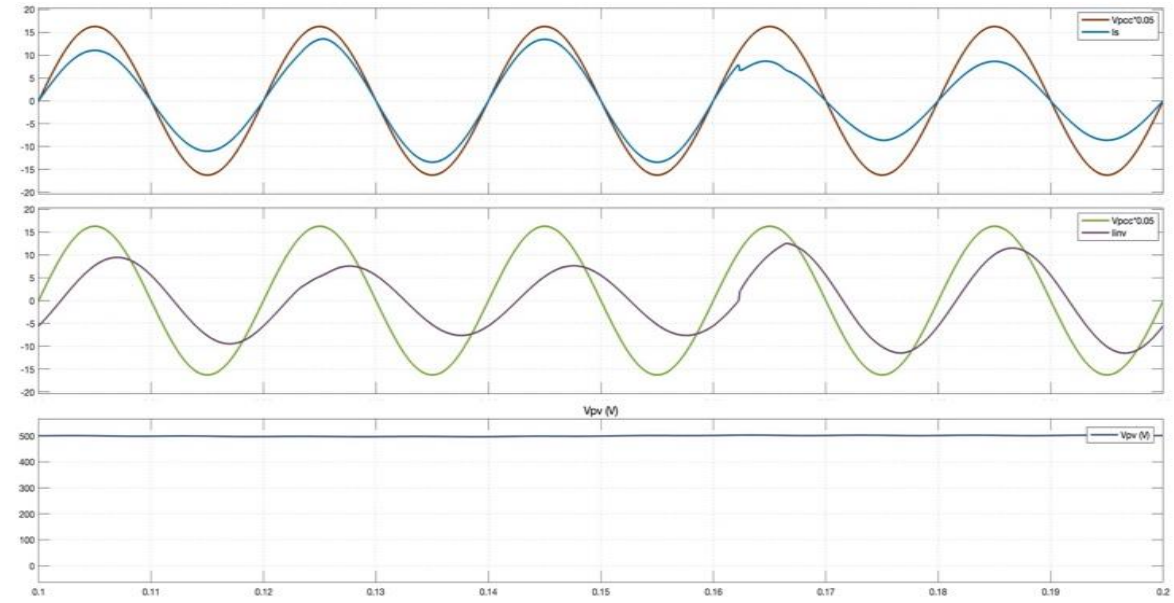

(a)

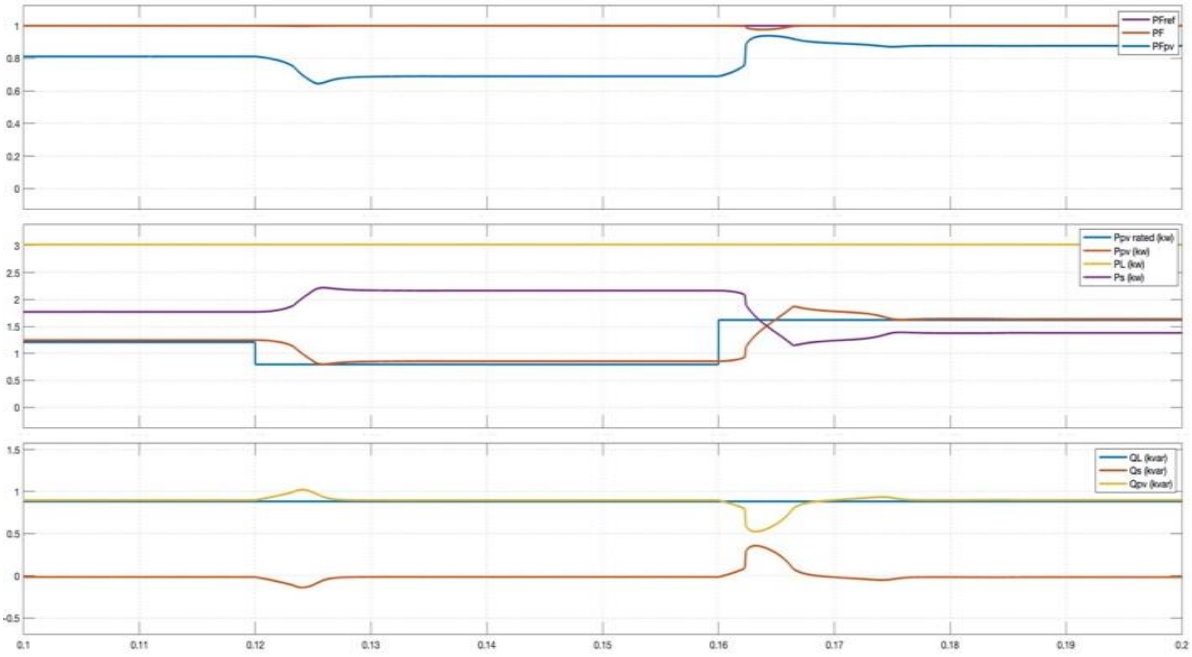

(b)

Fig. 21- (a) Voltage at PCC and DC side- Inverter and Source current. (b) P, Q, and PF of load, inverter, and source.

3.5 Conclusion

In this paper, a proposed control design of a grid-tied single-phase PV inverter system for power factor correction is presented. Employing MPPT the PV array maximum available power is injected into the grid. According to the simulation results, P and Q can be adjusted properly utilizing the suggested control strategy. The proposed control technique function is carried out for different radiation levels. The proposed controller responses to the different variation fast and is quietly stable when the transient period died out. It responds to the commands of PFC in less than 1ms. The results show that the controller can perform reactive power compensation and maintain the constant voltage at the grid satisfying standard for grid interconnection. This control strategy is appropriate for providing the grid with reactive power, therefore, can help customers avoid usage penalties by generating active power. They also can generate profits from selling reactive power to the grid since the PV system can operate throughout the day for 24 hours.

References

[1] B. K. Bose, "Global Warming: Energy, Environmental Pollution, and the Impact of Power Electronics," in IEEE Industrial Electronics Magazine, vol. 4, no. 1, pp. 6-17, March 2010, doi: 10.1109/MIE.2010.935860.

[2] H. Duz. " Storing solar energy inside compressed air through a heat machine mechanism,". Gazi Univ J Sci 2016;29.2:245e51.

[3] A. Scognamiglio, G. Adinolfi, G. Graditi and E. Saretta, "Photovoltaics in Net Zero Energy Buildings and Clusters: Enabling the Smart City Operation", Energy Procedia, vol. 61, pp. 1171-1174, 2014. Available: 10.1016/j.egypro.2014.11.1046.

[4] X. Li, H. Wen, L. Jiang, Y. Hu and C. Zhao, "An Improved Beta Method With Autoscaling Factor for Photovoltaic System", IEEE Transactions on Industry Applications, vol. 52, no. 5, pp. 4281-4291, 2016.

[5] C. Ramulu, P. Sanjeevikumar, R. Karampuri, S. Jain, A. Ertas and V. Fedak, "A solar PV water pumping solution using a three-level cascaded inverter connected induction motor drive", Engineering Science and Technology, an International Journal, vol. 19, no. 4, pp. 1731-1741, 2016. Available: 10.1016/j.jestch.2016.08.019.

[6] A. Cagnano, E. De Tuglie, M. Liserre and R. A. Mastromauro, "Online Optimal Reactive Power Control Strategy of PV Inverters," in IEEE Transactions on Industrial Electronics, vol. 58, no. 10, pp. 4549-4558, Oct. 2011, doi: 10.1109/TIE.2011.2116757.

[7] S. Balathandayuthapani, C. S. Edrington, S. D. Henry and J. Cao, "Analysis and Control of a Photovoltaic System: Application to a High-Penetration Case Study," in

IEEE Systems Journal, vol. 6, no. 2, pp. 213-219, June 2012, doi: 10.1109/JSYST.2011.2162889.

[8] S. Gonzalez, J. Neely and M. Ropp, "Effect of non-unity power factor operation in photovoltaic inverters employing grid support functions," 2014 IEEE 40th Photovoltaic Specialist Conference (PVSC), Denver, CO, 2014, pp. 1498-1503, doi: 10.1109/PVSC.2014.6925199.

[9] Wu L, Zhao Z, Liu J. Intelligent controller for solar lighting system. Tsinghua Univ J 2003;43(9):1195e8.

[10] W. Anthony, "Modeling and Analysis of a Photovoltaic System with a Distributed Energy Storage System," San Luis Obispo, M.Sc. Thesis, 2012.

[11] Y. Chen, C. Chang and H. Wu, "DC-link capacitor selections for the single-phase grid-connected PV system," 2009 International Conference on Power Electronics and Drive Systems (PEDS), Taipei, 2009, pp. 72-77, doi: 10.1109/PEDS.2009.5385801.

[12] R.Faranda and S. Leva, "Energy Comparison of MPPT Techniques for PV Systems", WSEAS Transactions on Power Systems , Vol. 3, No. 6, 2008, pp. 446-455

[13] V. Sineglazov and V. Kopanev, "SIMULATION MODELING OF SOLAR PLANTS WITH PHOTOELECTRIC CONVERTERS IN THE MODE OF SELECTION IN MAXIMUM POWER POINT IN MATLAB / SIMULINK", Electronics and Control Systems, vol. 1, no. 51, 2017. Available: 10.18372/1990-5548.51.11703.

[14] A.Yazdani and R. Iravani, Voltage-Sourced Converters: Modeling, Control, and Applications. Hoboken, NJ: Wiley, 2010.

Chapter 4: Low-Cost ESP32, Raspberry Pi, Node-Red, and MQTT Protocol Based SCADA System

This chapter is a paper accepted in IEMTRONICS 2020 conference and authored by Atefeh Zare and Dr. M. Tariq Iqbal, and was published on 2020 IEEE International IOT, Electronics and Mechatronics Conference (IEMTRONICS). The MEng candidate was involved with the planning and calculation of the experiments, method selection, the data analysis, and the writing of the paper.

4.1 Abstract

Growing energy cost and demand has motivated many organizations to achieve smart ways to monitor, control, and save energy. Smart automation can reduce costs while still satisfying energy demand. The residential, commercial, and industrial sectors can utilize the technologies of the Internet of Things (IoT) to manage energy consumption better. This paper presents a low-cost, open-source, and reliable Supervisory Control and Data Acquisition (SCADA) system for home monitoring and control system. The presented SCADA system consists of analog sensors, ESP32, Node-RED, and Message Queuing Telemetry Transport (MQTT) through local Wi-Fi to remotely access and control appliances. This system helps the users to monitor various conditions in the home, such as temperature, humidity, pressure, and light intensity. Thus, users can remotely monitor

various devices such as lights, fans, heating/cooling systems, make decisions based on the feedback of sensors.

4.2 Introduction and Literature Review

Nowadays, the fraction of automation systems in the residential sector is rising rapidly because of numerous life improvements such as comfort, convenience, centralized control of appliances, cost reduction, energy-saving, security, and safety. As a home automation system enhances the life quality for users, especially for the elderly, differently abled persons, and people who want to monitor and manage their home devices' operation, it is quietly important to have a proper control system. SCADA technologies implement a unique platform that senses and monitors remote devices, acquires data from them, and sends limited control instructions. Besides that, this system allows users to discover the status of devices and their residence conditions remotely.

Home automation systems using SCADA consists of four major parts. The first part is the sensing devices placed at several locations throughout the home to measure the desired variables. The second part is Remote Terminal Units (RTUs) for acquiring remote data from sensors. The third one is Master Terminal Units (MTUs) to process the received data and deal with Human Machine Interfaces (HMI) [1]. The last part of SCADA is the communication channel to connect the RTUs to the MTUs [2 ,3].

SCADA technology has been developed over the past years to remotely monitor and control processes. In this work, an open-source and low-cost SCADA system based on the Internet of Things is introduced. This SCADA system utilizes reliable and commonly available components to fulfill the four main functions of a SCADA system: Data

collection, network data communication, data presentation, and remote monitoring and supervisory control [4].

Several researchers around the world have designed SCADA systems based on IoT architecture in the past. Lekic et al. [5] performed an IoT-based SCADA system with the Raspberry Pi3. Temperature and humidity sensors acquired the desired data, and the IBM Bluemix cloud platform was utilized to receive, visualize, and manage the collected sensor data via the web while using the Node-Red and Web Socket protocols for data exchange and communication between the cloud platform and sensors connected to the Raspberry Pi.

In [6], Rai et al., Using IoT, implemented a system to provide the end-users with a cost-effective and portable intelligent monitoring system and enable devices remotely. The proposed system required a low-resolution video camera module interfaced with the Arducam ESP32 UNO board. The resulting video was streamed using ESP32 integrated Wi-Fi to display on the 1.8-inches SPI TFT Adafruit display module.

M. Al-Kuwari et al. [7] demonstrated sensing and monitoring platform on smart and IoT-based home automation system, where the authors presented a basic concept of how home automation can be deployed using IoT.

Pravalika et al. [8] implemented a home automation system through the Wi-Fi module, Massachusetts Institute of Technology (MIT) app, and a web page server using ESP32 to monitor home devices.

In [9], the MQTT-based home automation system using ESP8266 Node MCU was established for remote monitoring and controlling through a standard gateway. This system was designed utilizing the GSM (Global System for Mobile Communications) network.

In [10], Kodali demonstrated IoT-based smart environment monitoring using Arduino and C embedded programming devices, which were remotely controlled with the Internet. Temperature, humidity, light level, vibration, and air quality sensors connected to the controller for measurement and ESP8266 Node MCU for the Wi-Fi network.

Pujari et al. [11] demonstrated a smart home system that uses Wi-Fi to connect to the Internet, remotely monitor and control the appliances, and surveillance. Sensors were connected to ESP32 to collect data. All acquired data was uploaded to Firebase via the ESP32's built-in Wi-Fi, making it possible to control the home environment using the developed applications.

In [12], the IoT-based SCADA system proposed which the Raspberry Pi3 and Intel Edison board used for acquiring sensor inputs. Collected sensor data are transmitted to Amazon Web Services (AWS) through MQTT brokers in Node-Red. On the AWS IoT platform, several monitoring and control schemes inducted using Amazon's Voice Service named Alexa.

In this work, a low-cost and open-source SCADA system is developed that uses Wi-Fi, the MQTT protocol, and Node-Red. The proposed system can provide detailed measurements of temperature, pressure, humidity, and light density. Besides that, the states of the devices at home are being traced. Therefore, users can understand the status of their home devices such as lights, fans, air conditioners, or heating/cooling systems then remotely control them.

4.3 System Design

The proposed SCADA system block diagram is presented in Fig. 22. It is implemented using ESP32 as the sensor gateway and RTU and Raspberry Pi2 as a local server. SparkFun

Atmospheric Breakout Sensor-BME280 sensor and an LDR are connected to ESP32 to acquire the desired data and the dashboard to receive, visualize and manage the acquired sensors data over the web while using Node-Red and MQTT protocol for data exchange and communication between the MQTT clients such as end-users and the ESP32 connected sensors while the acquired data are being stored in SQLite as a web server. Each component is described in detail as following.

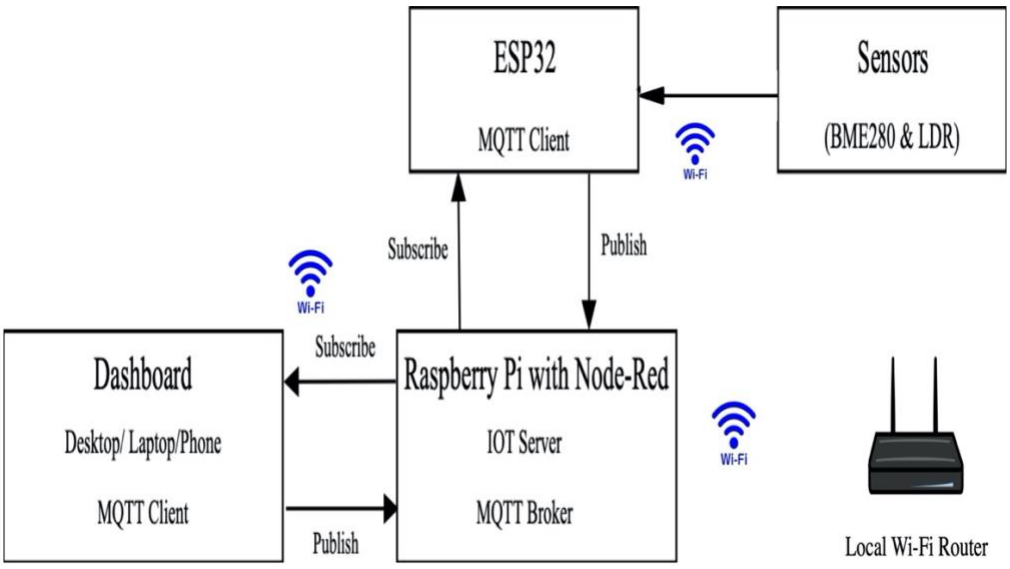

Fig. 22- The proposed SCADA system block diagram.

4.3.1 MQTT Communication Protocol

As shown in Fig. 23, MQTT is a publish/subscribe protocol. It is a lightweight and straightforward messaging tool designed for unreliable networks and constrained devices and low bandwidth. It is a suitable solution for this design since it provides simple

communication between the server (MQTT broker) and clients (ESP32 microcontroller and computers and mobile devices) [9-10, 13]. Clients can subscribe to the topics or publish the data to topics of any kind of data. The broker then distributes the data to any client that has subscribed to that topic. Eclipse Mosquitto software is being run as a broker on the local server (Raspberry Pi2).

In this project, the ESP32 microcontroller publishes the sensors data with specific topics to the MQTT broker (Mosquitto broker), while personal computers and mobile devices subscribe to the topics to visualize the published data on the server. MQTT protocol makes the supervisory control possible in this project.

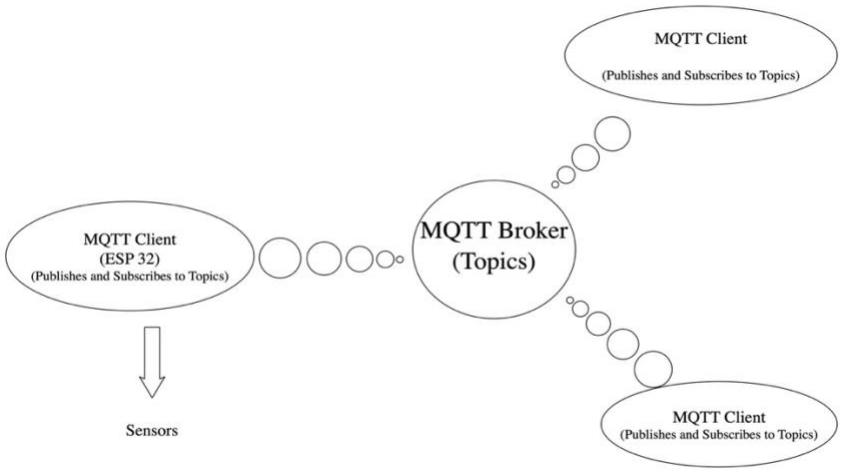

Fig. 23-MQTT Architecture

4.3.2 Raspberry Pi

The Raspberry Pi2 model B is used as the local server at a local network, including MQTT broker, Node-Red, SQLite.

4.3.3 ESP32 Thing

The ESP32 Thing is developed by SparkFun Electronics. It is one of the most low-cost, low-power, and small microcontrollers included Wi-Fi and Bluetooth modules. Fig. 24 shows a picture of the SparkFun ESP32 board.

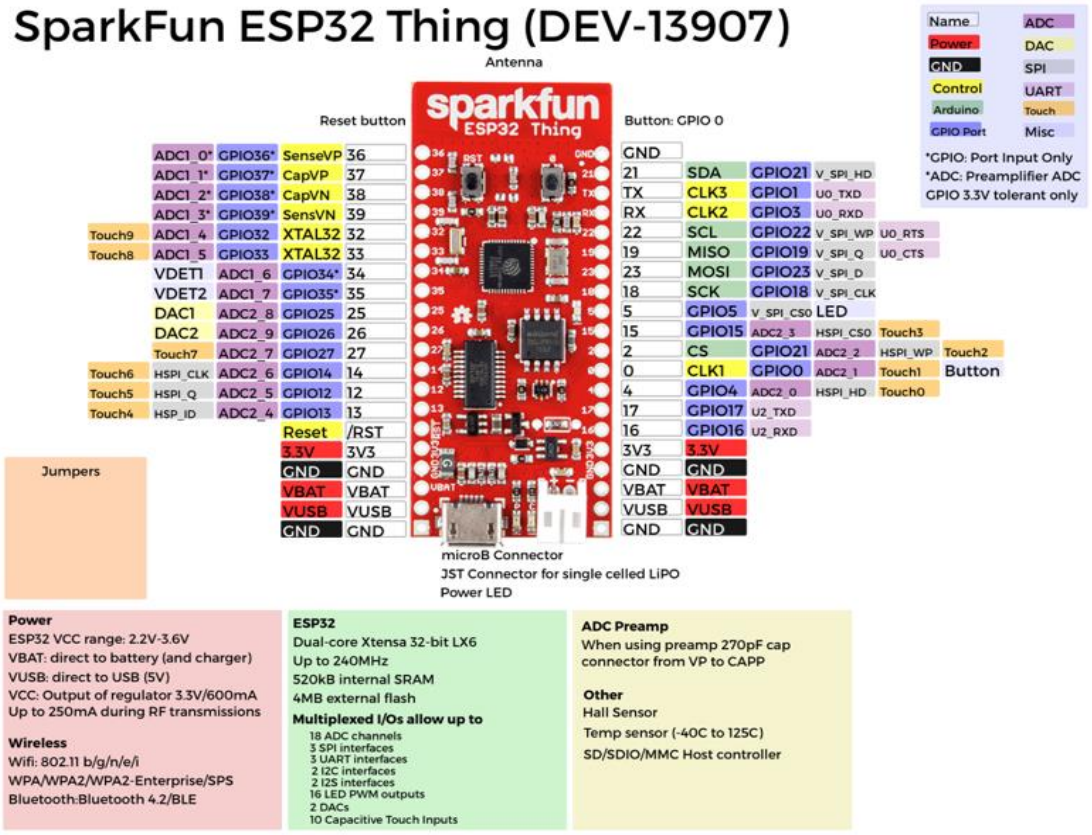

Fig. 24-Pin description of ESP32.

The board operating signal voltage range is 2.2 V to 3.6 V, and it can be supplied with either a 5 V USB power supply or with a battery. The microcontroller is programmed with

the Arduino software integrated development environment (IDE). The Arduino IDE allows experts to write the desired programs and upload them to the board via a USB cable. In this work, the ESP32 microcontroller is programmed as an MQTT client using the Arduino IDE software. The MQTT Client Library called PubSubClient. The program is such that the board collects the measured real-time values of desired variables, displays the values on the Arduino IDE Serial Monitor, and continuously publishes real-time data to the MQTT broker.

4.3.4 SparkFun Atmospheric Sensor Breakout BME280

The SparkFun BME280 Atmospheric Sensor Breakout is used to measure pressure, humidity, and temperature readings, all with a tiny breakout. It is shown in Fig. 25. The BME280 Breakout is designed to be deployed in indoor/outdoor navigation, home automation, etc. The on-board BME280 sensor measures atmospheric pressure, humidity, and temperature. The breakout presents a 5V tolerant I2C interface (with a pull-up resistor to 3.3V to be cooperative with ESP32).

Fig. 25- SparkFun Atmospheric Sensor Breakout BME280.

4.3.5 Light Dependent Resistor (LDR)

The LDR is a variable resistor. Fig. 26 presents LDR and its step-down resistor connection. The resistance of the LDR inversely proportionate to the light intensity. It shows maximum resistance in the absence of light and minimum resistance in the presence of light. Considering this characteristic, in this project, during the nighttime, LDR turns the LED ON and reversely makes the LED OFF during the daytime.

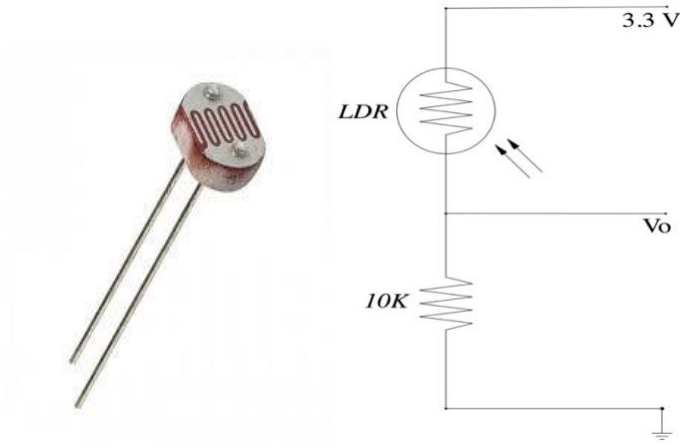

Fig. 26- LDR and its step-down resistor connection.

The relationship between the resistance RL and light intensity Lux for a typical LDR is [14]:

$$R_L = 500/Lux \qquad (4.1)$$

With the LDR connected to 3.3V through a 10K resistor, the output voltage of the LDR is:

$$V_O = (10*R_L)/(R_L+10) \qquad (4.2)$$

From equation (1) and (2), light intensity obtained as follows:

$$Lux = (500/V_O) - 50 \qquad (4.3)$$

The obtained Lux value is being used for controlling the LED.

4.3.6 Node-Red

Node-RED is an open-source programming tool used for wiring together hardware devices, APIs, and online services smartly [5]. It can be installed on a Linux-based platform, and it provides a browser-based editor that makes it easy to wire together flows using various nodes in the palette that can be deployed to its runtime.

4.3.7 Database and dashboard

An SQLite database using the litedb node on the Node-RED platform is installed to create database tables and store data. As a very lightweight relational database, SQLite does not need complex setup procedures, making it an ideal database management system to use for embedded systems and rapid prototyping. In this work, SQLite is set up to generate database, then stored data an easy-to-use dashboard (Node-Red dashboard) is used to display the acquired data from the data base.

Since the sensor data are published as MQTT messages to an MQTT broker, Arduino IDE sketch and Node-Red flow are used to transfer those MQTT messages and then store them in the database. Node-Red dashboard is a web-based data monitoring tool that can be combined to SQLite.

4.4 System Testing and Results

The home automation system's proposed design is used to monitor and control the house appliances while maintaining the minimum expected comfortable living conditions.

The flow chart of the proposed system is shown in Fig. 28. Accordingly, a prototype is shown in Fig. 27 is made to measure the desired variables. This prototype can be located in each room of the house. The sensors acquired data is being processed and used to control smart appliances such as smart LEDs, air conditioners, fans, etc.

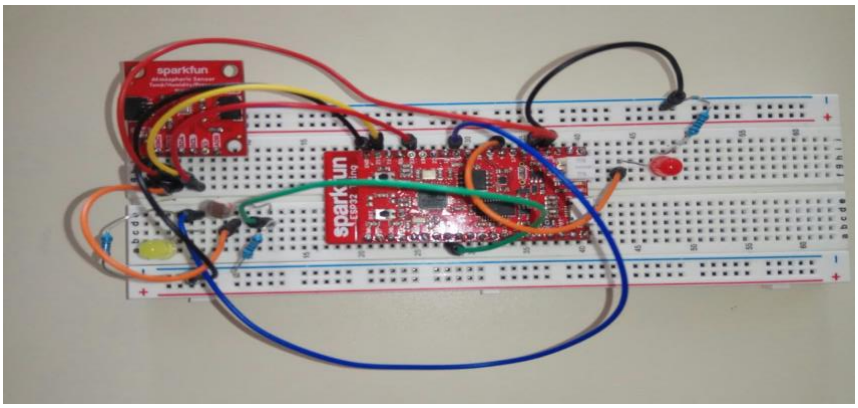

Fig. 27- Proposed SCADA system prototype.

In this project a yellow LED is used to test the automatic control ability of the system and a Red LED is implemented to evaluate the supervisory control capability of the proposed SCADA system.

This system monitors light intensity, temperature, humidity, and pressure values. If the recorded light intensity value goes beyond the set high or low value of the threshold level, the controller will generate the signal to turn the LED OFF/ON. Then the user will be notified by the LED status on the dashboard, this feature is presented in Fig. 29 and 30. As

shown in Fig. 29, the LDR is darken using a piece of paper to change the state of the LED which is presented in Fig. 30.

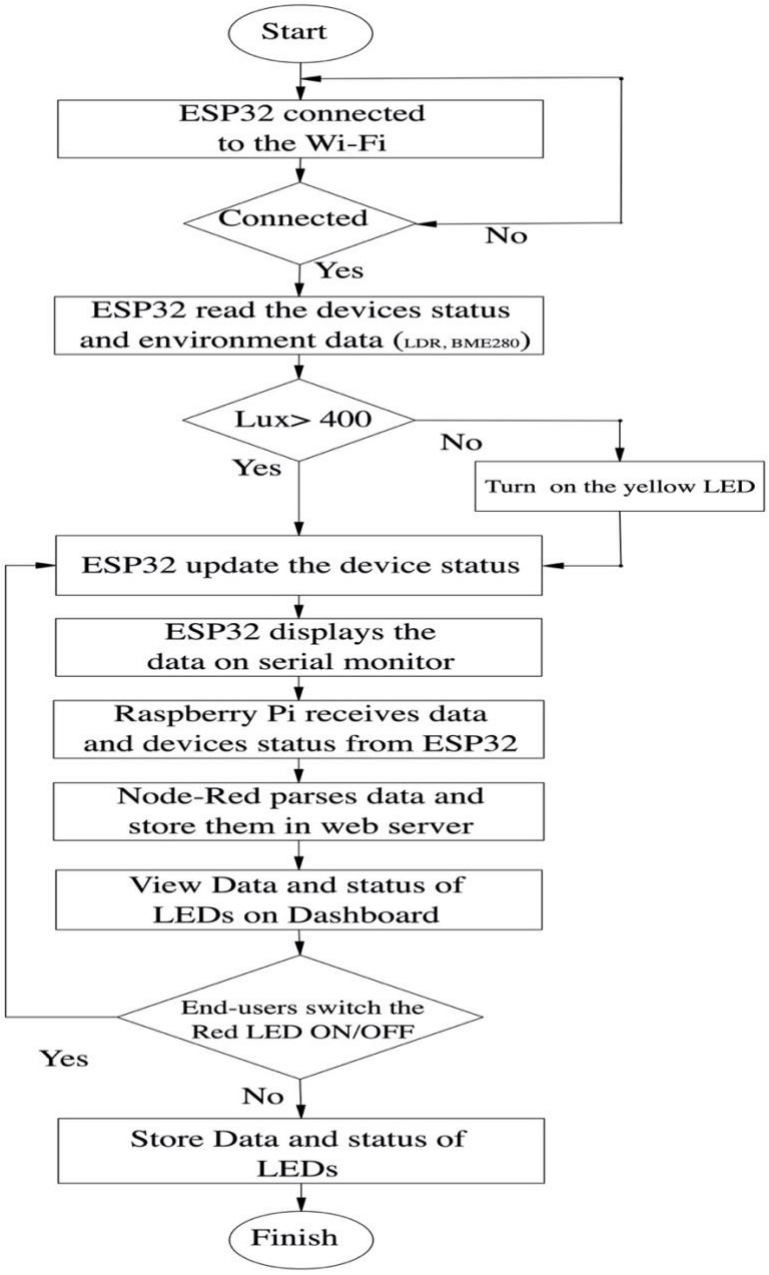

Fig. 28- The flow chart of the proposed SCADA system.

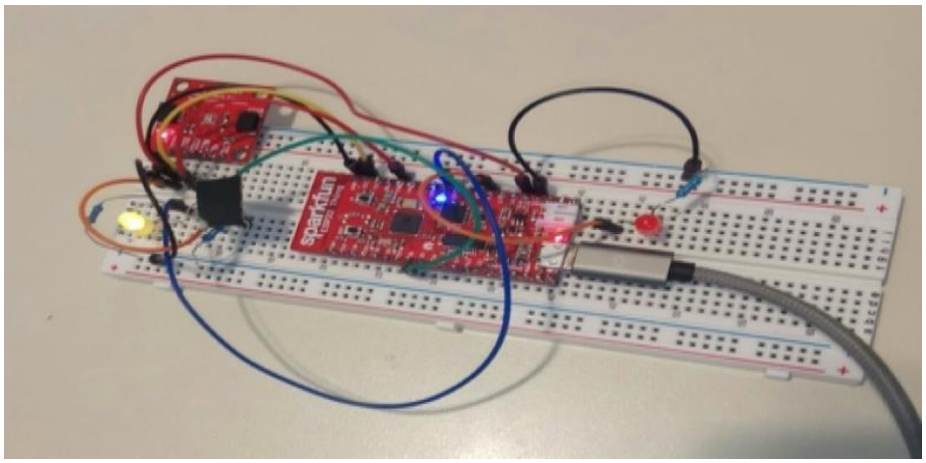

Fig. 29- The LED is turned on automatically based on the threshold value.

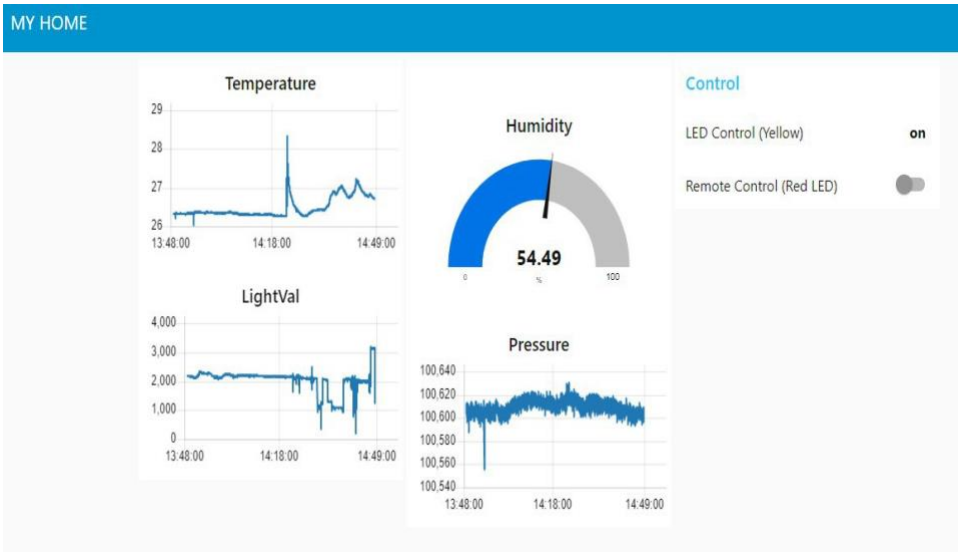

Fig. 30- The status of LED in Node-Red dashboard.

As mentioned earlier, the ESP32 controller subscribes to the published command, created by the end-user through the web interface, and transmitted by the Node-Red. Based on the received message, ESP32 sends a command to the LED to turn it ON/OFF

The implemented system is tested to evaluate its capability. Results provided in Fig. 31, 32 show the recorded values of temperature, humidity, and light density, and pressure, which are acquired and displayed over time through a data-viewing dashboard.

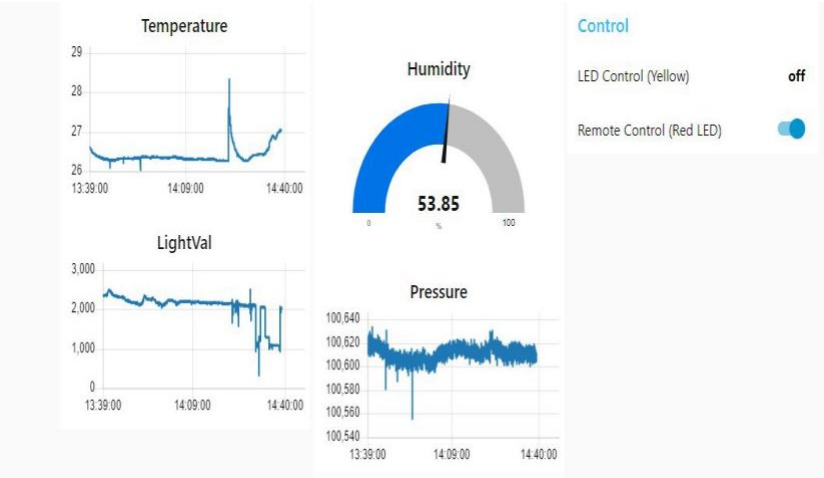

Fig. 31-The Red LED is controlled remotely by using Node-Red dashboard.

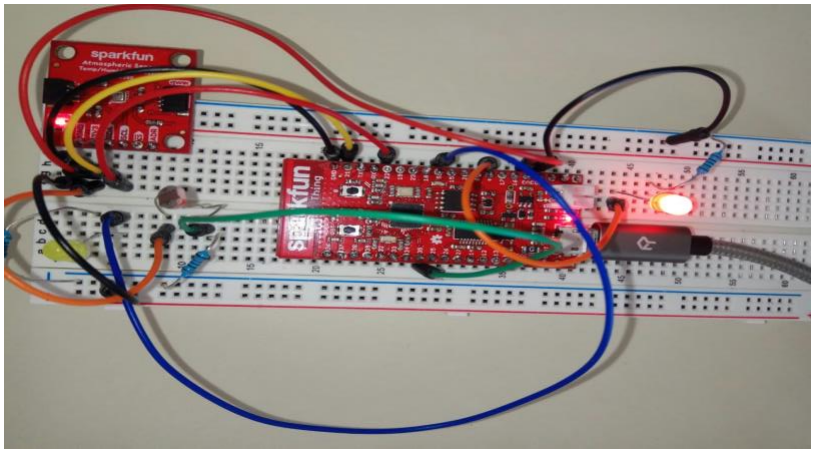

Fig. 32-The user remotely turned the Red LED on

4.5 Conclusions

The design of a low-cost and flexible and reliable IoT home automation system is presented. This proposed SCADA system is suitable for monitoring and controlling multi devices at home automatically and remotely. The system works in three phases. In the first one, the system monitors the temperature, pressure, humidity, and light intensity and uploads the data to database storage (SQLite) by using MQTT protocol and Node-Red installed on Raspberry Pi, then to the database connected dashboard. In the next phase, the system automatically controls the LED when the light intensity level exceeds the high or low predefined value of light intensity using a microcontroller (ESP32). In the last one, the supervisory control is achieved; the end-user can monitor and control the home devices through the web interface or mobile application. Once the message is sent through Node-Red along with the MQTT protocol to the microcontroller, it will be executed by ESP32 and turns the devices ON/OFF. The developed system cost is low, simple to operate, and is simply embedded with home devices.

References

[1] L. Amine and H. Abid, "Remote control of domestic equipment from an Android application based on Raspberry Pi card", IEEE transaction 15th international conference on Sciences and Techniques of Automatic control & computer engineering - STA'2014, Hammamet, Tunisia, December 21-23, 2014.

[2] B. S.S. Tejesh and S. Neeraja, "A Smart Home Automation system using IoT and Open-Source Hardware", International Journal of Engineering & Technology, vol. 7, no. 27, p. 428, 2018. Available: 10.14419/ijet.v7i2.7.10856.

[3] L. Aghenta and M. Iqbal, "Low-Cost, Open Source IoT-Based SCADA System Design Using Thinger.IO and ESP32 Thing", Electronics, vol. 8, no. 8, p. 822, 2019. Available: 10.3390/electronics8080822.

[4] A. Sajid, H. Abbas and K. Saleem, "Cloud-Assisted IoT-Based SCADA Systems Security: A Review of the State of the Art and Future Challenges", IEEE Access, vol. 4, pp. 1375-1384, 2016. Available: 10.1109/access.2016.2549047.

[5] M. Lekić and G. Gardašević, "IoT sensor integration to Node-RED platform," 2018 17th International Symposium INFOTEH-JAHORINA (INFOTEH), East Sarajevo, 2018, pp. 1-5, doi: 10.1109/INFOTEH.2018.8345544.

[6] P. Rai and M. Rehman, "ESP32 Based Smart Surveillance System," 2019 2nd International Conference on Computing, Mathematics and Engineering Technologies (iCoMET), Sukkur, Pakistan, 2019, pp. 1-3, doi: 10.1109/ICOMET.2019.8673463.

[7] M. Al-Kuwari, A. Ramadan, Y. Ismael, L. Al-Sughair, A. Gastli and M. Benammar, "Smart-home automation using IoT-based sensing and monitoring platform," 2018 IEEE 12th International Conference on Compatibility, Power Electronics and Power Engineering (CPE-POWERENG 2018), Doha, 2018, pp. 1-6, doi: 10.1109/CPE.2018.8372548.

[8] V. Pravalika and Ch. Rajendra Prasad, "Internet of Things Based Home Monitoring and Device Control Using Esp32", International Journal of Recent Technology and Engineering (IJRTE), vol. 8, no. 4, pp. 58-62, 2019.

[9] R. K. Kodali and S. Soratkal, "MQTT based home automation system using ESP8266," 2016 IEEE Region 10 Humanitarian Technology Conference (R10-HTC), Agra, 2016, pp. 1-5, doi: 10.1109/R10-HTC.2016.7906845.

[10] R. K. Kodali and S. Soratkal, "MQTT based home automation system using ESP8266," 2016 IEEE Region 10 Humanitarian Technology Conference (R10-HTC), Agra, 2016, pp. 1-5, doi: 10.1109/R10-HTC.2016.7906845.

[11] U. Pujaria, P. Patil, N. Bahadure and M. Asnodkar, "Internet of Things based Integrated Smart Home Automation System", SSRN Electronic Journal, 2020. Available: 10.2139/ssrn.3645458.

[12] A. Rajalakshmi and H. Shahnasser, "Internet of Things using Node-Red and alexa," 2017 17th International Symposium on Communications and Information Technologies (ISCIT), Cairns, QLD, 2017, pp. 1-4, doi: 10.1109/ISCIT.2017.8261194.

[13] K. Chooruang and P. Mangkalakeeree, "Wireless Heart Rate Monitoring System Using MQTT", Procedia Computer Science, vol. 86, pp. 160-163, 2016. Available: 10.1016/j.procs.2016.05.045.

[14] D. NAGARAJU, C. KIREET, N. KUMAR and R. JATOTH, "Performance Comparision Of Signal Conditioning Circuits For Light Intensity Measurement", World Academics Journal of Engineering Sciences, vol. 01, no. 02, pp. 2007 (1-10), 2014. Available: 10.15449/wjes.2014.2007.

Chapter 5: Summary and conclusion

5.1 Research Summary

Small renewable power systems have attracted more attention in today's power generation systems, mainly due to the increasing energy demand and the quest for cleaner energy sources. PV power generation systems can be used widely in most parts of the world. However, in some countries non-renewable energy sources are being used to produce power. In Iran, homes are using the generated electricity from non-renewable resources. In this research the PV and load size are estimated to achieve a high efficiency, low cost, and environment friendly operation and installation of renewable energy system. This system supplemented by remote monitoring and control technologies is more attractive and easier to utilize. Supervisory control and data acquisition (SCADA) systems make this coordination possible. However, to use the microgrids, the need for dynamic modeling of the systems also is inevitable.

This thesis presented an investigation in literature on renewable energy, especially photovoltaic systems. It presented that Iran is blessed with a significant amount of solar energy which can be used as a clean energy resource.

Based on literature search, this thesis presented the design of a grid-connected and a standalone PV power system for a house in Iran. To make the design more accurate, the amount of load demand was estimated using BEopt software. Then a PV/grid and a PV/diesel/battery were proposed and carried out by HOMER software. Based on the cost

analysis and carbon emission results the PV/grid system was selected as a power generation system.

The dynamic model of grid-connected single-phase PV system was then built in MATLAB /SIMULINK to check the performance of the system. The proposed control system consists of an incremental conductance MPPT controller, a DC bus voltage controller and a current controller. The current controller consists of two PI controllers to achieve the active and reactive control based on the reference power factor. The simulation results demonstrate that the proposed control design has a fast response to MPPT control and maintains the whole system steady-state operation under various circumstances such as variation in solar irradiance and power factor. The results also present that the proposed controller can extract the maximum power from the PV under various solar radiation, perform reactive power compensation and maintain the constant voltage at the point of common coupling. The proposed system is a candidate for reactive power support to the utility grid. This system can also help customers avoid usage penalties while generating revenues from the sale of real power. Thus, the PV solar system can be entirely utilized for a full 24-hour period.

A low-cost and flexible and reliable SCADA system were designed and tested for remote monitoring and controlling a household. The designed open-source SCADA system used the Internet of Things (IoT), the most recent SCADA architecture. The proposed SCADA system was implemented using ESP32 as the sensor gateway and RTU and Raspberry Pi2 as a local server, BME280 sensor and an LDR connected to ESP32 to acquire the desired data and the dashboard to receive, visualize and manage the acquired sensors data over the web while using Node-Red and MQTT protocol for data exchange and communication

between the MQTT clients. The proposed SCADA system was tested extensively. The results demonstrate that the system performed optimally and accurately.

5.2 Future Work

- Add the wind turbine to the designed power system for the selected house for higher renewable penetration.
- Develop a wiring system by Helioscope
- Add switches and breakers to the system for the protection and safety proposes.
- Develop the designed SCADA system to monitor and control other systems remotely.
- To make the designed SCADA system more attractive, some dashboards can be designed by the developer to be charge free.
- Develop a data analysis based on the obtained data

5.3 Publications

[1] A. Zare, M. T. Iqbal, "Low-Cost ESP32, Raspberry Pi, Node-Red, and MQTT Protocol Based SCADA System," *2020 IEEE International IOT, Electronics and Mechatronics Conference (IEMTRONICS)*, Vancouver, BC, Canada, 2020, pp. 1-5, doi: 10.1109/IEMTRONICS51293.2020.9216412.

[2] A. Zare and M. Iqbal, “Dynamic Modeling and Control of a Single-Phase Grid-Connected photovoltaic System”, *EJECE*, vol. 4, no. 6, Dec. 2020.

[3] A. Zare and M. T. Iqbal, “Optimal Sizing of a PV System in Golpayegan, Iran Using Thermal Modeling-based Load Demand”, *EJERS, vol. 5, no. 12, pp. 152-156, Dec. 2020.*

[4] A. Rehman, H. Elsaraf, A. Zare, and M. Tariq Iqbal, “Design and analysis of a rooftop PV system for an apartment building in Newfoundland,” *Accepted for presentation at the 29th IEEE NECEC 2019, St. John’s, NL, Canada. November 19, 2020.*